Geological Magazine

www.cambridge.org/geo

Original Article

Cite this article: Yin J, Liang C, Zheng C, Song Z, Jia X, and Chen L. The final closure time of the eastern segment of the Paleo-Asian Ocean: Insights from geochronology and geochemistry of Permian-Triassic sedimentary sequence in Wangqing, Jilin Province, China. *Geological Magazine* **161**(e22): 1–18. https://doi.org/10.1017/S0016756824000359

Received: 16 June 2024
Revised: 3 September 2024
Accepted: 17 October 2024

Keywords:
provenance analysis; zircon U-Pb dating; geochemistry; Paleo-Asian Ocean; Central Asian Orogenic Belt

Corresponding author:
Chenyue Liang;
Email: chenyueliang@jlu.edu.cn

The final closure time of the eastern segment of the Paleo-Asian Ocean: Insights from geochronology and geochemistry of Permian-Triassic sedimentary sequence in Wangqing, Jilin Province, China

Junzhe Yin[1], Chenyue Liang[1,2], Changqing Zheng[1,2], Zhiwei Song[1], Xianghe Jia[1] and Long Chen[1]

[1]College of Earth Sciences, Jilin University, Changchun, China and [2]Key Laboratory of Mineral Resources Evaluation in Northeast Asia, Ministry of Natural Resources, Jilin University, Changchun, China

Abstract

The Central Asian Orogenic Belt is the world's largest accretionary orogenic belt, associated with the closure of the Paleo-Asian Ocean (PAO). However, the final closure timing of the eastern PAO remains contentious. The Permian-Triassic sedimentary sequences in the Wangqing area along the Changchun-Yanji suture zone offer important clues into this final closure. New data on petrology, whole-rock geochemistry, zircon U-Pb geochronology and zircon Hf isotopes of sedimentary rocks from the Miaoling Formation and Kedao Group in Wangqing area provide new insights into the final closure of the eastern end of the PAO. The maximum deposition ages of the Miaoling Formation and Kedao Group have been constrained to the Late Permian (ca. 253 Ma) and early Middle Triassic (ca. 243 Ma), respectively. These sedimentary rocks exhibit similar geochemical characteristics, showing low textural and compositional maturities, implying short sediment transport, with all detrital zircons suggesting their origins from felsic igneous rocks. The $\varepsilon_{Hf}(t)$ values of the Miaoling Formation range from −6.09 to 12.43 and from −2.20 to 7.59 for the Kedao Group, implying these rocks originated from NE China. Considering our new data along with previously published data, we propose that a reduced remnant ocean remained along the Changchun-Yanji suture zone in the early Middle Triassic (ca. 243 Ma), suggesting the final closure of the eastern PAO likely occurred between the latest Middle Triassic and early Late Triassic.

Highlights:

1. Miaoling Formation and Kedao Group were deposited around 253 Ma and 243 Ma, respectively.
2. The eastern segment of the Paleo-Asian Ocean closed in a scissor-like manner along the Changchun-Yanji suture zone.
3. Remnants of the Paleo-Asian Ocean still existed in the early Middle Triassic.

1. Introduction

The Central Asian Orogenic Belt (CAOB), the largest accretionary orogenic belt on Earth, is situated between the Siberian Craton to the north, and the North China and Tarim Cratons to the south (Sengör et al. 1993; Windley et al. 2007; Wilde, 2015; Xiao et al. 2015; Xu et al. 2015; Chen et al. 2022; Li, H.D. et al. 2022; Fig. 1a) and reflects a complex tectonic evolution closely connected to the closure of the Paleo-Asian Ocean (PAO) (Khain et al. 2002; Windley et al. 2007; Xiao et al. 2015; Zhang et al. 2019; Wu et al. 2007; Pei et al. 2016). Northeastern China (NE China), also called the Xing'an-Mongolian Orogenic Belt (XMOB; Sun et al. 2004; Xu et al. 2014), is located in the eastern segment of the CAOB and has witnessed the amalgamation of NE China massifs during Paleozoic and early Mesozoic, which from west to east are Erguna, Xing'an, Songnen and Jiamusi-Khanka massifs or terranes, all of which are separated by major faults or suture belts (Wu et al. 2007, 2011; Zhou et al. 2011a, b, 2015; Zhou & Wilde, 2013; Cao et al. 2012, 2013; Santosh & Somerville, 2013; Sun et al. 2013; Xu et al. 2014; Mi et al. 2017; Liu et al. 2017; Li, 2006; Tang et al. 2013; Fig. 1a). This amalgamation of NE China (XMOB) and the North China Craton (NCC) along the Solonker-Xar Moron-Changchun-Yanji Suture (SXCYS) is commonly recognized as the final closure of the PAO, supported by evidence from magmatic rocks, structural features and palaeontological data (Sun et al. 2004; Jia et al. 2004; Wu et al. 2007; Cao et al. 2013; Zhou et al. 2017; Wang et al. 2015a, b; Li et al. 2017; Yang et al. 2017; Gu et al. 2018; Du et al. 2019). Nonetheless, there are still no definite conclusions about the final

https://doi.org/10.1017/S0016756824000359 Published online by Cambridge University Press

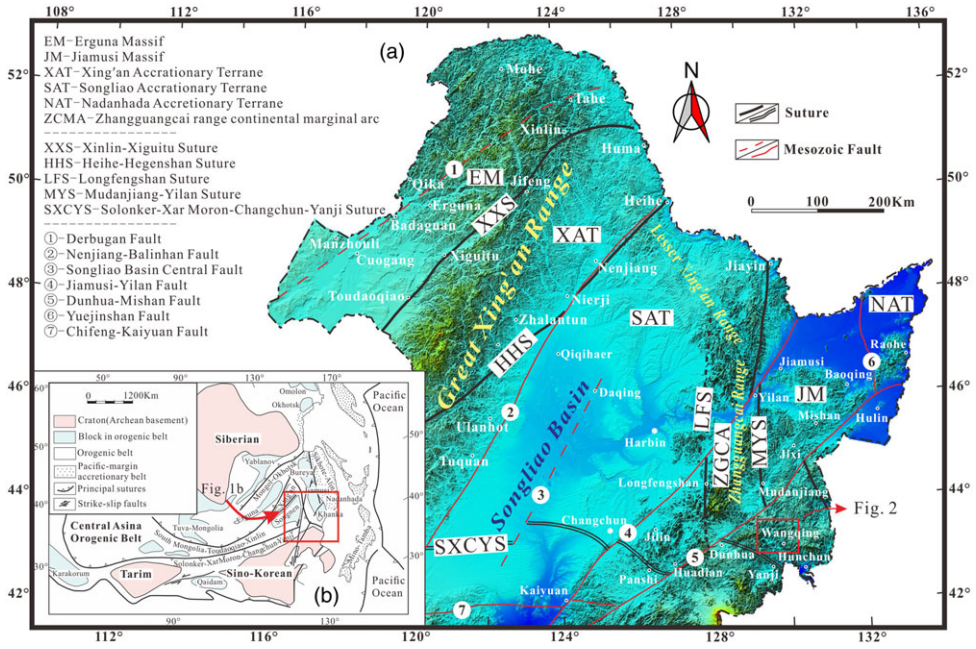

Figure 1. Tectonic sketch map of the Central Asian Orogenic Belt (a; Zhou & Wilde, 2013) and NE China (b; Liu et al. 2017).

closure time of the PAO, as different scholars present varied perspectives. The closing process of the PAO during the Permain-Triassic has been inferred through the study of intrusive rocks exposed in the NCC and igneous rocks in NE China (Cao et al. 2013; Guan et al. 2022; Han et al. 2020, 2021; Song et al. 2018; Wang et al. 2015b; Wu et al. 2007; Yuan et al. 2016; Yu et al. 2022). Some scholars, using high-quality paleomagnetic data and geological evidence, suggest the closure around 250 Ma (Zhao et al. 2013; Ren et al. 2023). Conversely, others, focusing on sedimentary rocks, argue differently (Du et al. 2019, 2021; Han et al. 2019; Liu J et al. 2017; Shi et al. 2020; Sun et al. 2022; Wang et al. 2015a). Most studies agree that the final suturing occurred during the Permian-Triassic (Cao et al. 2013; Du et al. 2019, 2021; Guan et al. 2022; Han et al. 2019, 2020, 2021; Li, 2006; Li & Zhao, 2007; Liu J et al. 2017, 2020; Shi et al. 2020; Song et al. 2018; Sun et al. 2022; Wang et al. 2015a, b; Wu et al. 2007; Yuan et al. 2016), while some propose it occurred before the Permian (Zhang et al. 2008; Shi et al. 2010), or even before the Late Devonian (Xu & Chen, 1997; Zhao et al. 2013; Xu et al. 2015; Zhu & Ren, 2017), or between the Late Devonian and Early Carboniferous (Tang, 1989; Hong et al. 1995). Others suggest that closure spanned from the Permian to Triassic, encompassing late Early Permian (Yu et al. 2022; Feng et al. 2010; Liu et al. 2010), Middle to Late Permian(Sengör et al. 1993; Chen et al. 2000, 2009; Jian et al. 2010; Lin et al. 2013), Late Permian (Li, 2006; Wu et al. 2011), Late Permian to Early Triassic (Sengör et al. 1993; Li, 1998, 2006; Xiao et al. 2003; Sun et al. 2004; Zhang et al. 2004; Wu et al. 2007, 2011; Xu et al. 2009; Peng et al. 2012; Cao et al. 2013; Eizenhöfer et al. 2014; Li et al. 2014; Wilde, 2015; Han et al. 2015; Guo et al. 2016; Wu & Li, 2022), Late Permian to Middle Triassic (Jia et al. 2004; Wang F et al. 2015; Xiao et al. 2015; Liu et al. 2017; Guan et al. 2023) and Middle-Late Triassic (Peng et al. 2012; Zhou & Wilde, 2013). This controversy largely arises from insufficient time constraints and sedimentological data for the transition from subduction to collision in the eastern segment of CAOB (Zhang et al. 2023).

This uncertainty about the provenance of Late Permian to Triassic sedimentary rocks in this area and the absence of constraints from related orogenic events further exacerbate the differing viewpoints. The Wangqing area in eastern Jilin Province, adjacent to the Changchun-Yanji suture zone, plays a key area in elucidating the final closure of the eastern end of PAO (Fig. 2). This study focuses on petrology, geochronology and geochemistry investigations conducted on sandstone samples from the Middle Permian Miaoling Formation and Upper Triassic Kedao Group in the Wangqing area, aiming to enhance the understanding of the evolution and closure history of the eastern PAO from a perspective of provenance analysis.

2. Geological setting and sample descriptions

2. a. Geological setting

The SXCYS is bordered by the eastern CAOB to the north and the NCC to the south. NE China is located in the east segment of the CAOB, also known as the XMOB, which consists of numerous micro-blocks, including the Erguna Block, Xing'an Block, Songnen-Zhanggaungcai Range and Jiamusi-Khanka massifs or terranes (Ge et al. 2005; Huang et al. 2006; Li, S.K. et al. 2020). The NCC, the oldest and largest known craton in China, is divided into the Western Block and the Eastern Block, which amalgamated along the Trans-North China Orogen around 1.85 Ga (Zhao et al. 2012). Jilin Province features a series of discontinuous Permian-Triassic sedimentary sequences along the Changhun-Yanji suture, witnessing the amalgamation of NE China blocks and the NCC, preserved within the extensive "granite ocean" (Cao et al. 2013). The study area in the Wangqing area in the east of Jilin Province, adjacent to the southeastern XMOB and the northern NCC (Fig. 1a), is pivotal in reconstructing the final closure process of the PAO and the collision between the NCC and NE China.

The tectonic evolution history of NE China is complex, featuring Phanerozoic granitoids and Paleozoic to Mesozoic sediments, such as the Middle Permian Miaoling Formation and the Triassic Kedao Group. Intrusions associated with the PAO tectonic domain are primarily I-type granites and mafic to ultramafic rocks, while those related to the Paleo-Pacific tectonic

https://doi.org/10.1017/S0016756824000359 Published online by Cambridge University Press

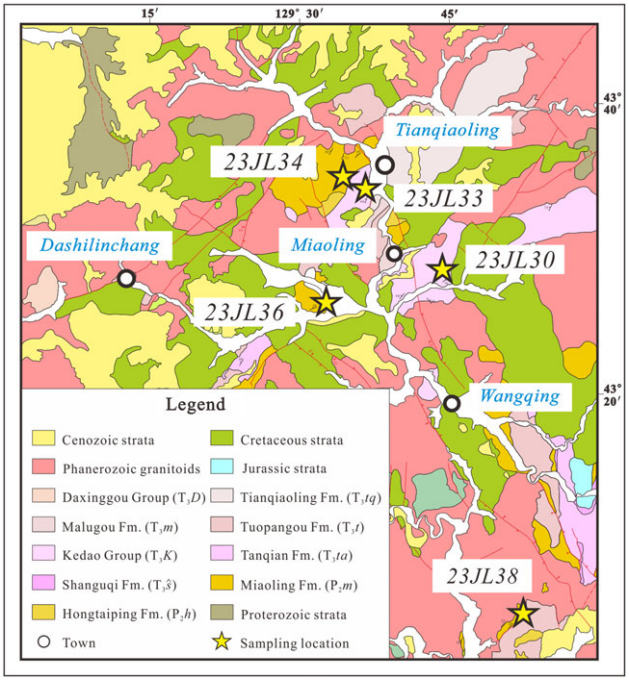

Figure 2. Detailed geological map of the Wangqing area showing the stratigraphic distribution and sampling locations.

domain consist mainly of A-type and I-type granites, with fewer mafic intrusions. Different formations often exhibit distinct lithological characteristics and different fossil assemblages. Previous studies on the Miaoling Formation have focused on volcanic interlayers (Lu et al. 2022), while the definition of the Kedao Group remains unclear (Yu, 2017). Therefore, for our study, we select the Miaoling Formation and the Kedao Group in the Wangqing area, Jilin Province, as our sampling locations are closer to the Changchun-Yanji suture zone, providing better representation.

Sun (1988) defined the Miaoling Formation as marine siliceous pyroclastic rocks intercalated with intermediate-felsic lavas, siltstone and limestone lenses. It exhibits a conformable contact with the upper Hongtaiping Formation and an angular unconformable contact with the lower Kedao Group. Its lower part is predominantly composed of grey and grey-green feldspathic quartz sandstone, greywacke and siltstone, intercalated with thin lenses of limestone; the upper part is mainly characterized by sandstone, siltstone and shale, interbedded with thick lenses of limestone.

Yin et al. (2011) concluded that the Kedao Group consists of Permian marine strata, divided into the Shanguqi and the Tanqian formations, which are mainly composed of fluvio-lacustrine deposits. Its upper part is in parallel unconformity with the Daxinggou Group, and the lower part is in angular unconformity with the Miaoling Formation. This group consists mainly of conglomerate, tuffaceous siltstone, arkose and shale with intercalated allochthonous limestone blocks (Shen et al. 2019; see Fig. 3 for more details).

2. b. Sample descriptions

Five samples were collected in the study area (Fig. 2), including mudstone 23JL34, grey-black mudstone 23JL36 and graywacke 23JL38 from the Miaoling Formation and grey-black siltstone 23JL30, blueish-grey mudstone 23JL33 from the Kedao Group.

2. b.1. Miaoling formation

Samples 23JL34 (43°34′57.35″N, 129°34′0.75″E) and 23JL36 (43°25′36.77″N, 129°32′16.37″E) are both mudstones with over 90% argillaceous content; the primary difference is their colour under microscope, with 23JL34 appearing yellow-brown (Fig. 4a and d) and 23JL36 grey-black (Fig. 4b and e).

Sample 23JL38 (43°3′12.36″N, 129°51′48.77″E) is a graywacke from Shixian town, characterized by low maturity, with 50% matrix and 50% clastic fragments, featuring 70% quartz, 5% polycrystalline quartz and 25% feldspar, with poorly sorted, sub-rounded grains and aligned mineral fragments (Fig. 4c and f).

2. b.2. Kedao group

The Kedao Group is dominantly exposed in Miaoling, Kedao, Xiangrenping, Houdidong, Wangqing and Sidonggou in the Yanbian area, with an exposed area of approximately 189 km^2 (RGSR, 2007). Predominantly composed of conglomerate and tuffaceous siltstone, these strata contain few fossils and exhibit contested age estimates (BGMRJP, 1997). While some studies suggest a Permian origin (BGMRJP, 1997), recent evidence indicates an Early-Middle Triassic age, supported by Triassic fossils (Zhou, 2009) and geochronologic data from the Yanji area.

Sample 23JL30 (43°27′53.65″N, 129°43′24.31″E) is a grey-black siltstone from the eastern Miaoling Quarry, characterized by low maturity and composed of 35% matrix and 65% clastic fragments. It comprises 80% quartz and 20% feldspar, featuring a clastic texture with poorly sorted, sub-rounded grains and a clear alignment of mineral fragments (Fig. 5a and c).

Sample 23JL33 (43°34′0.38″N, 129°36′3.54″E) is a blueish-grey mudstone in the southwest of Tianqiaoling town, containing over 90% argillaceous materials and presenting challenges for mineral identification (Fig. 5b and d).

3. Analytical methods

3. a. LA-ICP-MS zircon U-Pb dating

Selected zircon grains (Fig. 6) were mounted into an epoxy resin disc and polished to about half-sections to expose grain interiors. Cathodoluminescence (CL) images coupled with transmitted and reflected light micrographs were obtained to examine the internal structures. Zircon U-Pb isotopic and trace element analyses were performed using an ASI^{TM} RESOlution-LR Series 193 nm excimer laser ablation instrument (LA) coupled with Thermo Scientific^{TM} iCAP^{TM} RQ series inductively coupled plasma mass spectrometry (ICP-MC) at Key Laboratory of Orogen and Crust Evolution, Peking University and Hebei Key Laboratory of Strategic Critical Mineral Resources, Hebei GEO University. The laser spot diameter is 29μm, the frequency is 6 Hz and the energy density is 3 J/cm^2. High-purity argon gas is used as the carrier gas and high-purity He and N_2 gas are used to increase sensitivity. The background of ^{204}Pb and ^{202}Hg is usually less than 100 cps. Calibration for the zircon U/Pb ratios and trace elements was carried out by using the standard zircon 91500 (1062 Ma; Wiedenbeck et al. 1995) and glass standard NIST 610, respectively. Zircon standard Plésovice (337 Ma; Sláma et al. 2008) and GJ-1 are also used to supervise the deviation of age measurement/calculation. Those external standards were analyzed once per five unknown samples. The contents of trace elements in all zircons were also calculated using 91Zr as an internal standard. Isotopic ratios and element concentrations of zircons were calculated using GLITTER (ver. 4.4.2, Macquarie University) and iolite ver. 4.3.0. The common lead was corrected

https://doi.org/10.1017/S0016756824000359 Published online by Cambridge University Press

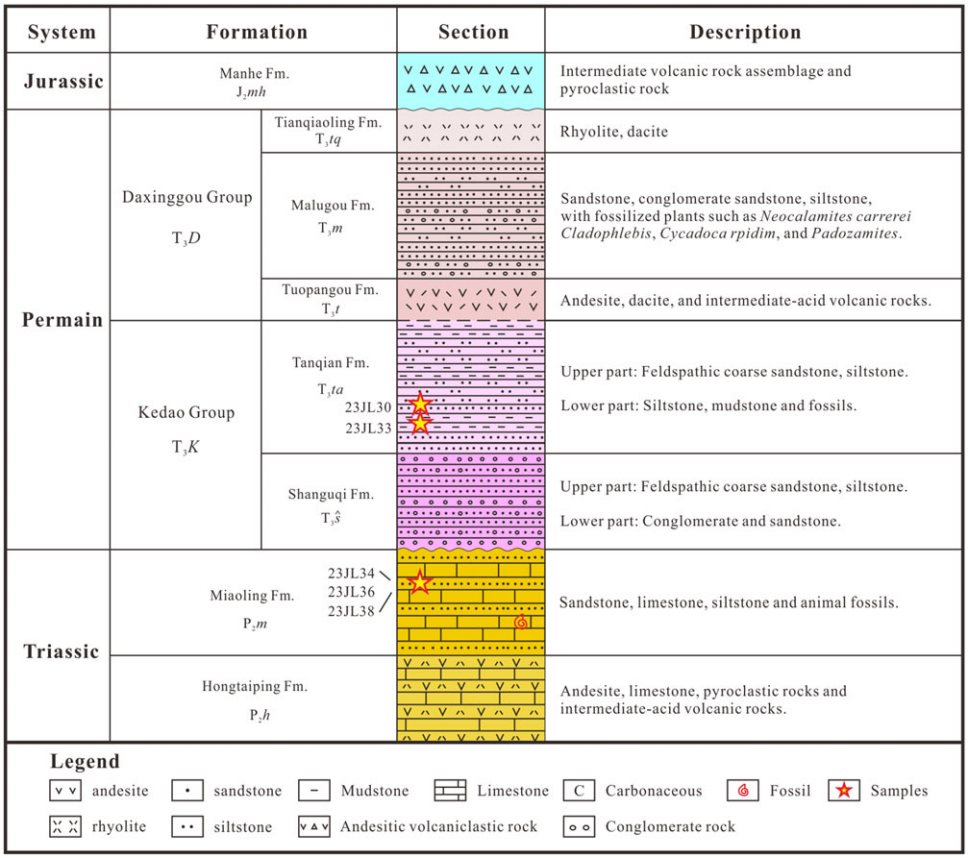

Figure 3. Stratigraphic columns of the study area with sampling locations.

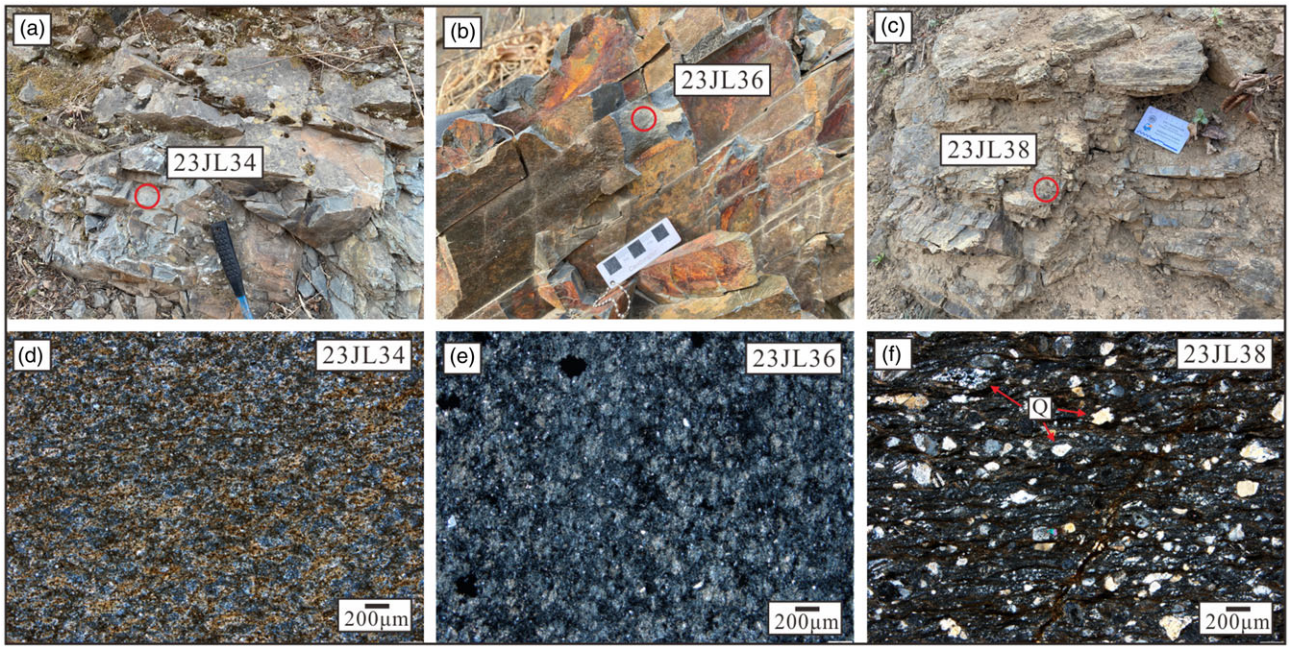

Figure 4. Field photographs (a-c) and photomicrographs (d-f) of analyzed samples from the Miaoling Formation.

using LA-ICP-MS Common Lead Correction (ver. 3.15), following the method of Anderson (2002). Concordia diagrams and weighted average plots were obtained using Isoplot/Ex (3.0) (Ludwig, 2003). Probability density distribution plots were produced using AgeDisplay (Sircombe, 2004). Uncertainties on individual analyses are reported at the 2σ and mean ages for pooled U/Pb analyses are calculated at a 95% confidence interval.

All the errors are within 2σ interval, and the isotopic ages plotted in the diagrams for the relative probability of the ages of the samples. The $^{207}Pb/^{206}Pb$ age is used when the age is over 1000 Ma,

https://doi.org/10.1017/S0016756824000359 Published online by Cambridge University Press

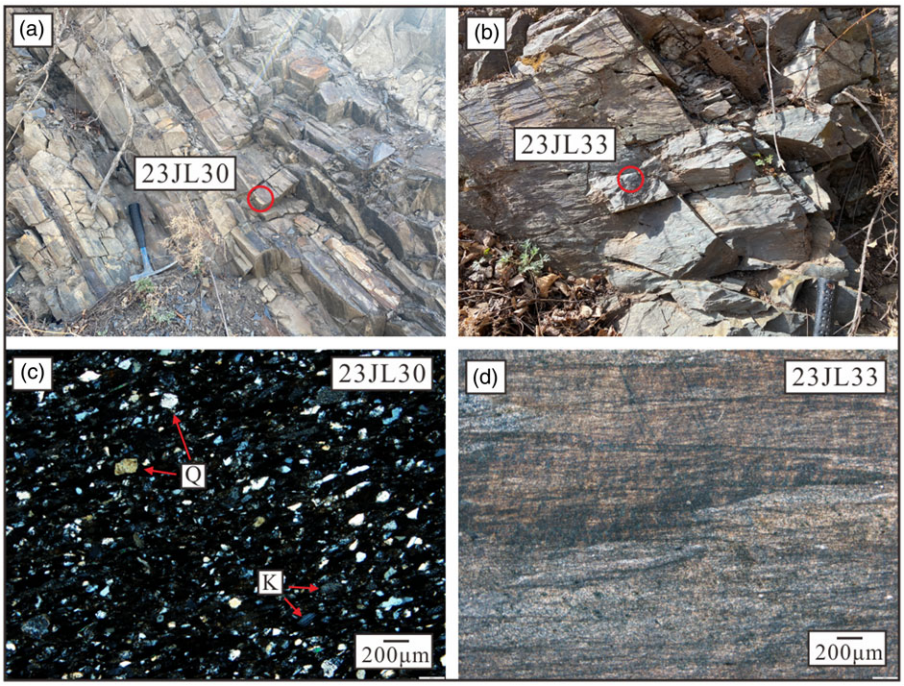

Figure 5. Field photographs (a-b) and micrographs (c-d) of analyzed samples from the Kedao Group.

Figure 6. Cathodoluminescence (CL) images of representative detrital zircons from all dated samples. Circles mark dating spots (red for U-Pb isotopic tests, yellow for Hf isotopic tests.). Below zircons refer to the U-Pb ages, above are dating numbers.

while the $^{206}Pb/^{238}U$ age is used when the age is younger than 1000 Ma due to the imprecise measurement of ^{207}Pb in young grains (Sircombe, 1999). The ages with discordance degree over 10% were excluded when Mapping.

3. b. Major and trace element determinations

The siltstone samples used for whole-rock analysis were crushed to ~200 mesh in an agate mill after the removal of altered surfaces. Major and trace elements compositions were determined by using an X-ray fluorescence spectrometer and ICP-MS (Agilent 7700x), respectively, at the Key Laboratory of Mineral Resources Evaluation in Northeast Asia, Ministry of Natural Resources, Jilin University, Changchun, China, after the sample powders had been dissolved in Teflon bombs. The analytical results for the BHVO-1 (basalt), BCR-2 (basalt) and AGV-1 (andesite) standards yielded values of analytical precision that were better than 5% for major elements and 10% for trace elements (Rudnick et al. 2004).

3. c. Hf isotope analysis

Zircon Hf isotope ratios were measured using a Neptune (Plus) MC-ICP-MS (ThermoFisher Scientific^{TM}, USA) equipped with an ASI^{TM} RESOlution-LR Series 193 nm excimer laser ablation instrument, which is hosted at the Hebei Key Laboratory of Strategic Critical Mineral Resources, Hebei GEO University, China. These analyses were performed with a laser beam diameter of ca. 43 μm and 5 Hz repetition rate, yielding a signal intensity of ~1.2 v at ^{179}Hf during the analysis of the standard zircon GJ-1. The ablation time is 40 s, yielding pits of 30–40 μm deep. Masses 172, 173, 175, 176, 177, 178, 179 and 180 were simultaneously measured in static-collection mode. Standard zircons GJ-1 were

https://doi.org/10.1017/S0016756824000359 Published online by Cambridge University Press

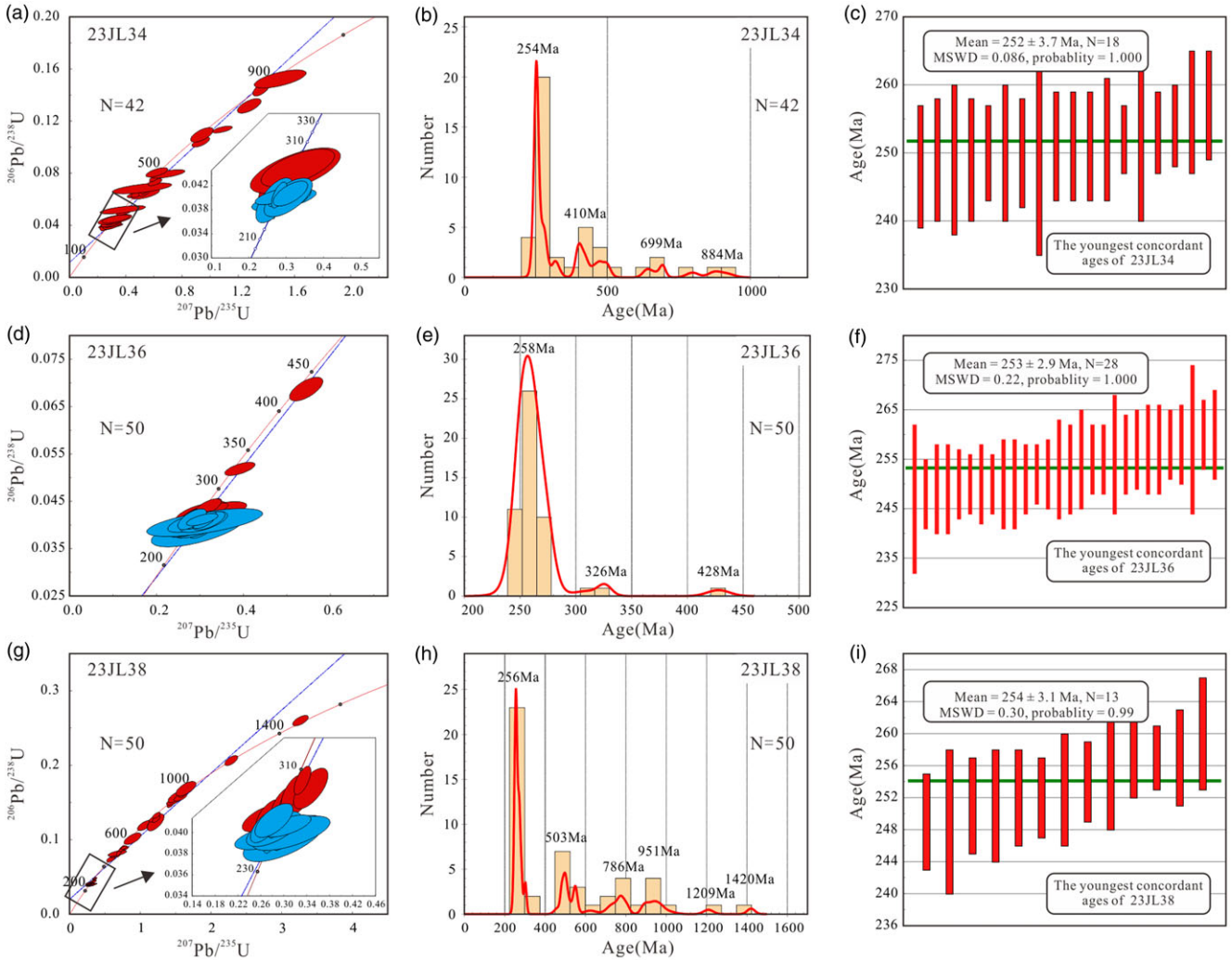

Figure 7. U-Pb concordia diagrams of detrital zircons from the Miaoling Formation; ellipses represent 2σ uncertainties (blue ellipses represent the group of the youngest concordant ages).

used as external standards and were analyzed twice before and after every 10 analyses. The resulting data were normalized to $^{179}Hf/^{177}Hf = 0.7325$ using an exponential correction for mass bias. The interference of ^{176}Lu on ^{176}Hf was corrected by measuring the intensity of the interference-free ^{175}Lu isotope and using the recommended $^{176}Lu/^{175}Lu$ ratio of 0.02655. The mean $^{173}Yb/^{172}Yb$ ratio on the zircon sample itself was measured to calculate the mass fractionation factor β_{Yb}, and the signal intensity of ^{176}Yb was calculated based on the signal intensity of ^{173}Yb and the calculated β_{Yb}, and then used to correct the interference of ^{176}Yb on ^{176}Hf.

4. Analytical results

4. a. Zircon U–Pb dating

4. a.1. Miaoling formation

A total of 142 concordant U-Pb dating analyses from three samples in this study were obtained, and the results are given in Supplementary Table 1. All dated zircons, ranging in size from 30–220 μm, are euhedral to subhedral with some corrosion marks (Fig. 6). Their high Th/U ratios of 0.02–2.17 (over 98% are above 0.1) and clear oscillatory zones (Fig. 6) indicate a magmatic origin (Wu & Zheng, 2004).

In sample 23JL34, 42 zircon grains yield concordant ages ranging from 248 ± 9 Ma to 915 ± 26 Ma (Fig. 7a; Supplementary Table 1), grouped as 248–284 Ma (42 grains, peaking at 254 Ma), 316–500 Ma (12 grains, peaking at 410 Ma) and 638–915 Ma (6 grains) (Fig. 7b). The youngest ages yield the $^{206}Pb/^{238}U$ weight mean age of 252 ± 3.7 Ma (Fig. 7c; Mean Square Weighted Deviation (MSWD) = 0.086, n = 18), with a mean Th/U ratio of 0.64.

In sample 23JL36, 50 concordant zircons show concordant ages from 247 ± 15 Ma to 428 ± 10 Ma (Fig. 7d; Supplementary Table 1), predominantly in the age group of 247–276 Ma (47 grains, peaking at 258 Ma) (Fig. 7e). The youngest zircons yield the $^{206}Pb/^{238}U$ age of 253 ± 2.9 Ma (Fig. 7f; MSWD = 0.22, n = 28), with a mean Th/U ratio of 0.53.

For sample 23JL38, 50 zircon grains yield concordant ages from 249 ± 6 Ma to 1420 ± 19 Ma (Fig. 7g; Supplementary Table 1), which can be subdivided into groups of 249–303 Ma (25 grains, peaking at 256 Ma), 463–553 Ma (10 grains, peaking at 503 Ma) and 623–1420 Ma (15 grains) (Fig. 7h). The youngest zircons yield the $^{206}Pb/^{238}U$ weight mean age of 254 ± 3.1 Ma (Fig. 7i; MSWD = 0.30, n = 13), with a mean Th/U ratio of 0.57.

https://doi.org/10.1017/S0016756824000359 Published online by Cambridge University Press

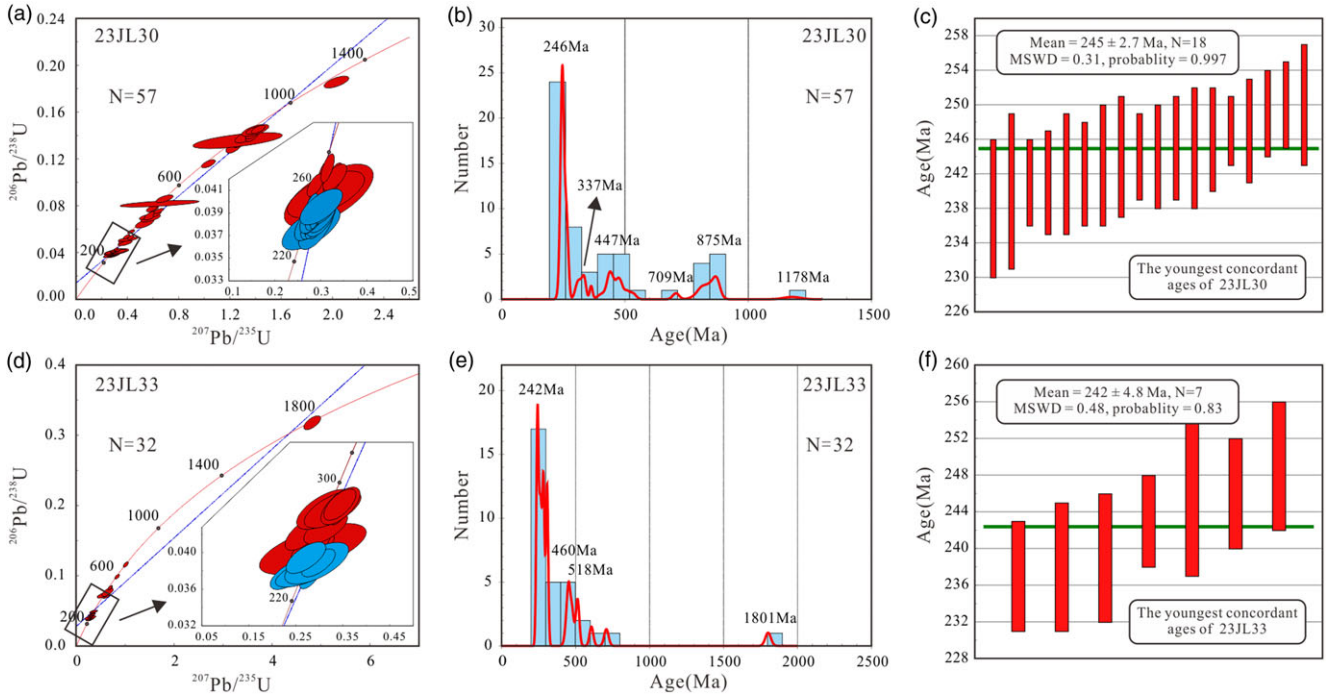

Figure 8. U-Pb concordia diagrams for detrital zircons from the Kedao Group; ellipses represent 2σ uncertainties (blue ellipses represent the group of the youngest concordant ages).

4. a.2. Kedao group

A total of 89 concordant U-Pb dating analyses from two samples in this study were obtained, and the results are given in Supplementary Table 1. All dated zircons, ranging in size from 30 to 200 μm, are euhedral to subhedral with some corrosion marks (Fig. 6). They exhibit high Th/U ratios of 0.08–2.13 (over 98% are above 0.1) and clear oscillatory zones (Fig. 6), indicating a magmatic origin (Wu & Zheng, 2004).

For sample 23JL30, 57 zircons yield concordant ages ranging from 238±8 Ma to 1178±34 Ma (Fig. 8a; Supplementary Table 1), falling into groups of 238–271 Ma (29 grains, peaking at 246 Ma), 303–363 Ma (6 grains, peaking at 337 Ma), 405–532 Ma (11 grains) and 707–1178 Ma (11 grains) (Fig. 8b). The youngest concordant zircon yields the $^{206}Pb/^{238}U$ age of 245 ± 2.7 Ma (Fig. 8c; MSWD = 0.31, n = 18), with a mean Th/U ratio of 0.52.

For sample 23JL33, 32 concordant zircons yield a broad age spectrum ranging from 237 ± 6 Ma to 1801 ± 19 Ma (Fig. 8d; Supplementary Table 1), which can be divided into groups of 237–310 Ma (22 grains, peaking at 242 Ma), 445–708 Ma (9 grains, peaking at 460 Ma and 518 Ma) and 1801 Ma (Fig. 8e). The youngest zircons with a mean Th/U ratio of 0.66 yield the $^{206}Pb/^{238}U$ age of 242±4.8 Ma (Fig. 8f; MSWD = 0.48, n = 7).

4. b. Major and trace elements

4. b.1. Major elements

Whole-rock major and trace elemental analyses were carried out on the fifteen sandstones and the data are provided in Supplementary Table 2. Samples from the Miaoling Formation have higher contents of $^{T}Fe_2O_3$, CaO, MgO, Na_2O, Ti_2O, P_2O_5 and MnO, but lower contents of SiO_2, Al_2O_3 and K_2O than those from the Kedao Group. The SiO_2/Al_2O_3 ratios are relatively low (3.13–5.68; average 3.92), classifying the samples as immature rocks (Peittijohn et al. 1972; Herron, 1988). In the lithological discrimination (Fig. 9), all samples from both formations are plotted in the greywacke area, consistent with our microscopic observations (Figs. 4 and 5).

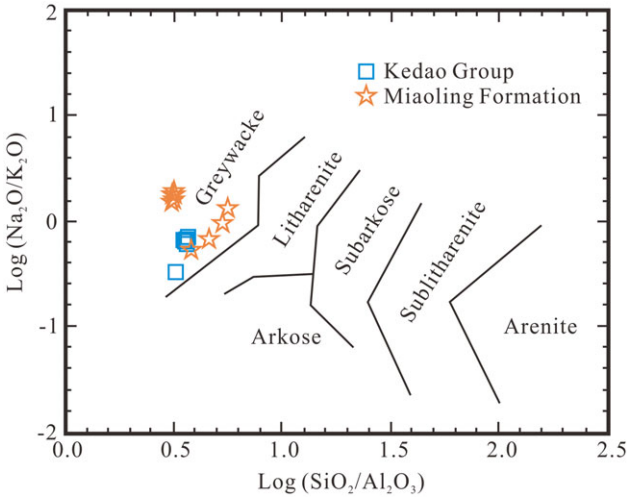

Figure 9. Geochemical classification diagrams of the Miaoling Formations and Kedao Group (after Pettijohn et al. 1972 and Herron, 1988).

4. b.2. Trace elements

The chondrite-normalized Rare Earth Elements (REEs) distribution patterns of all samples are similar to those of the average upper continental crust (Rudnick & Gao, 2014), featuring enriched Light Rare Earth Elements (LREEs) ($(La/Yb)_N$ = 1.79–7.13; averagely 4.29), flat Heavy Rare Earth Elements (HREEs) ($(Gd/Yb)_N$ = 0.95–2.42; averagely 1.45) and slight to moderate negative Eu anomalies (Fig. 10a), with no Ce anomaly. The

https://doi.org/10.1017/S0016756824000359 Published online by Cambridge University Press

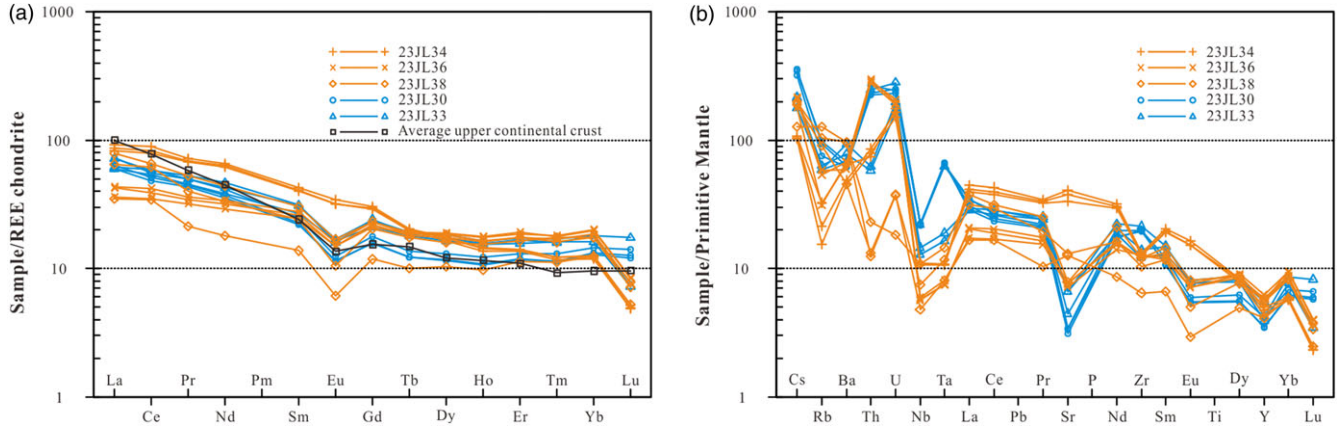

Figure 10. Chondrite-normalized REE patterns (left) and Primitive Mantle trace element diagrams (right) for the studied sandstones. The normalizing values for REE and trace elements are from McDonough & Sun (1995) and Boynton (1984), respectively. Data for the average upper continental crust are from Rudnick & Gao (2014).

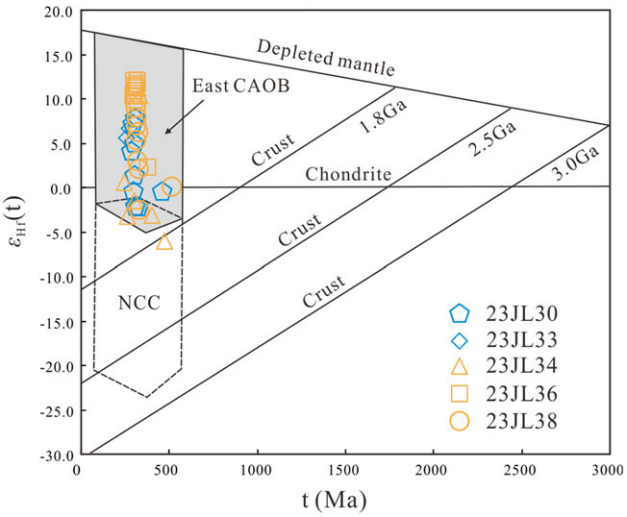

Figure 11. Hf isotopic compositions of detrital zircons from Miaoling Formation (yellow) and Kedao Group (blue) in the study area (Yang et al. 2006).

enrichment of LREEs and depletion in HREEs are obvious for all samples, reflected in their similar right-dipping curves. The mantle-normalized multi-element variation diagram of trace elements shows a consistent trend (Fig. 10b), indicating depletion of high-field strength elements (HFSE) Nb, Ta and of large-ion lithophile elements Sr, while showing slight enrichment in Ba, Th, La, Ce, Nd, and Sm in HFSE and Zr, K in large-ion lithophile elements, although the enrichment of La and Ce is not conspicuous.

4. c. Hf Isotope results

We conducted Hf isotope analysis on representative Paleozoic to Mesozoic zircon grains from sedimentary rocks of the Miaoling Formation and Kedao Group (Supplementary Table 3 and Fig. 11).

The Hf isotopic compositions of 28 detrital zircons from the Miaoling Formation (23JL34, 23JL36 and 23JL38) were analyzed. Paleozoic zircons (495–254 Ma) exhibit $^{176}Hf/^{177}Hf$ ratios ranging from 0.2823145 to 0.2829695, with $\varepsilon_{Hf}(t)$ values varying between −6.09 and 12.43, and the T_{DM2} are 1830–493 Ma. Mesozoic zircons (251–247 Ma) exhibit $^{176}Hf/^{177}Hf$ ratios ranging from 0.282512 to 0.282947, with $\varepsilon_{Hf}(t)$ values varying between -3.90 and 11.5, and the T_{DM2} ranging from 1272 to 488 Ma (Supplementary Table 3).

The Hf isotopic compositions of 12 detrital zircons from the Kedao Group (23JL30 and 23JL33) were analyzed. Paleozoic zircons (438–252 Ma) exhibit $^{176}Hf/^{177}Hf$ ratios ranging from 0.2824738 to 0.282837, with $\varepsilon_{Hf}(t)$ values varying between -2.20 and 7.59, and the T_{DM2} of 1499–794 Ma. Mesozoic zircons (250–239 Ma) exhibit $^{176}Hf/^{177}Hf$ ratios ranging from 0.2825632 to 0.282849, with $\varepsilon_{Hf}(t)$ values varying between -2.07 and 7.66, and the T_{DM2} of 1407–784 Ma (Supplementary Table 3).

5. Discussion

5. a. The sedimentary ages of the miaoling formation and kedao group

The deposition time of a sedimentary strata is much younger than its sediments, allowing detrital zircons within a formation to help constrain the maximum deposition ages (Fedo, 2003). This method relies on the assumption that the U-Pb system of analyzed zircons remained undisturbed by post-depositional tectonic-metamorphic or hydrothermal events (Zeh & Gerdes, 2012). In this study, combined with age-diagnostic fossils and intruded dykes, the mean age of the youngest overlapping zircon grains at 2σ uncertainty (Dickinson & Gehrels, 2009) was used to estimate the maximum deposition ages of the Miaoling Formation and Kedao Group in Wangqing area.

5. a.1. Miaoling formation

Extensive research has been conducted on the Miaoling Formation; however, its deposition time remains a point of contention. Gathering all data from these three samples (23JL34, 23JL36 and 23JL38), the maximum depositional age of the Miaoling Formation was determined to be late Permian by the 57 youngest concordant zircons having a weighted mean $^{206}Pb/^{238}U$ age of 253 ± 1.9 Ma (Fig. 14d; MSWD = 0.19, n = 57). Among all 142 concordant zircons, only 21 are older than 600 Ma, with the oldest three grains yielding the $^{207}Pb/^{206}Pb$ age of 1005 ± 36 Ma, 1209 ± 24 Ma and 1420 ± 19 Ma (Fig. 14c). Phanerozoic ages peak at 256 Ma (Fig. 14c). This late Permian maximum depositional age is obviously younger than the previously published youngest cluster of zircons in sandstones with the age of ca. 265 Ma (Lu et al. 2022).

https://doi.org/10.1017/S0016756824000359 Published online by Cambridge University Press

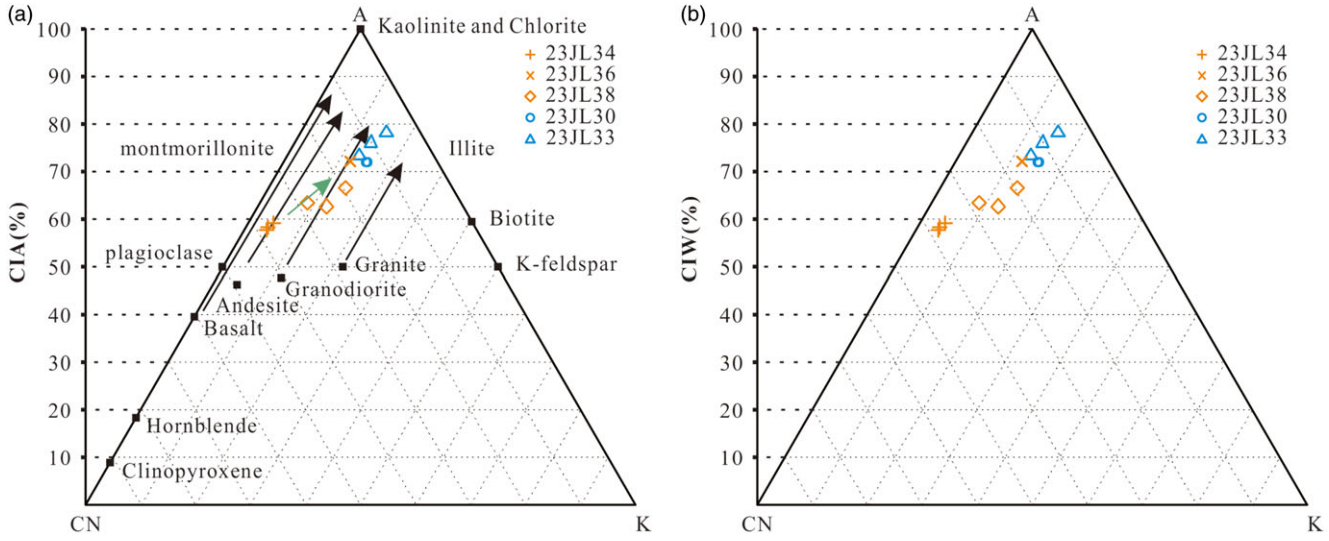

Figure 12. A-CN-K weathering diagram of major elements (after Nesbitt & Young, 1984) in sandstones from the Wangqing area. The solid arrow represents the ideal weathering trend line of each igneous rock, according to data from Condie (1993). A: Al_2O_3, CN: CaO^*+Na_2O, K: K_2O.

5. a.2. Kedao group

Divergent views exist regarding the sedimentary ages of the Kedao Group, ranging from the Late Permian to the Late Triassic (Zhou, 2009; Yu, 2017; Zhou et al. 2017; Du et al. 2019). Combining all the data from two samples together, the 20 youngest concordant zircons of the Kedao Group yielded a weighted mean $^{206}Pb/^{238}U$ age of 243 ± 2.7 Ma (MSWD = 0.24, n = 20) (Fig. 14b), implying the maximum depositional age of Middle Triassic (ca. 243 Ma). Precambrian zircons constitute a significant proportion in all analyses (15.7%), with 14 grains older than 600 Ma, while the Phanerozoic ages with peaks of 245 Ma and 468 Ma (Fig. 14a).

5. b. Provenance analysis of Miaoling Formation and Kedao Group in the study area

The chemical index of alteration (CIA) is useful for quantitatively assessing weathering intensity (Fedo et al. 1995; Nesbitt & Young, 1984). The samples show an average CIA value of 68.60, reflecting weak initial chemical weathering (Fig. 12a; Fedo et al. 1995). In the A-CN-K diagram (Fig. 12b), the average Chemical Index of Weathering is 77.85, about 10% higher than the CIA. The weathering trend deviates slightly to the right (Fig. 12a), indicating a potassium metasomatism influence during diagenesis, which indicates a nearby source and a short transportation distance. The intersection of the weathering trend line and the plagioclase-K-feldspar line indicates a higher plagioclase content than K-feldspar in parent rocks (Fedo et al. 1995), indicating a provenance related to felsic igneous. Analyzed detrital zircons, in this study, show a positive correlation between U and Y concentrations, suggesting origins from intermediate-acidic igneous rocks such as granite, syenite and pegmatite. The trace element analysis of zircons also indicates that the parent rocks were primarily felsic igneous, although some points suggest minor mixture of mafic rocks (Fig. 13a, b, c, and d). Overall, these characteristics indicate that the REE contents of the sandstones approximate the global average for continental upper crust, with their provenance related to felsic rocks in the upper crust.

Both the sandstones from Miaoling Formation and Kedao Group exhibit characteristics of greywackes (Figs. 4, 5, and 9), with low compositional and textural maturities indicating a nearby provenance. These samples contain a high proportion of argillaceous materials and various sizes of mineral clasts. The CL images of euhedral detrital zircons further support a relatively near source. Possible provenance areas for these formations include the NCC to the south and the NE China massifs (Zhangguangcai Range and Jiamusi-Khanka block) to the north (Fig. 1a). Detrital zircons carry geochronological information about their source rocks and have high diagenesis stability (Wu & Zheng, 2004), providing them a valuable for provenance analysis of sandstones at plate margins or orogenic belts.

The age distributions of these two formations exhibit the same characteristics, as evidenced by variations in the proportion of each age group and the distribution of peak ages (Fig. 14). The Miaoling Formation is characterized by the overwhelming majority of Phanerozoic zircons (81.3%), with 118 out of 145 grains. A peak age of ca. 256 Ma can be perfectly related to the Permian granitic magmatism (256–252 Ma; Yu et al. 2013) and magmatic activities linked to the westward subduction of an ancient oceanic plate in the southern Jiamusi-Khanka block (272–257 Ma; Long et al. 2019). A peak age of ca. 504 Ma is consistent with the ~500 Ma late Pan-African crystal basement in NE China massifs (Xiong et al. 2020; Hua et al. 2019; Li, Y. et al. 2017; Wen et al. 2017; Wang et al. 2012; Wu et al. 2011; Yang et al. 2014; Zhou et al. 2011b, 2015, 2018), representing typical differences from the NCC. In addition, a minor peak at 920 Ma in the Neoproterozoic is consistent with the magmatic activities in NE China, implying a strong affinity. Both the Kedao Group and Miaoling Formation exhibit similar magmatic activity peaks at 245 Ma, 468 Ma and 876 Ma, while zircon grains older than 1000 Ma are rare in both formations, lacking distinct peaks, which highlights a clear deviation from the zircon curve of the NCC (Fig. 14).

Vermeesch (2013) proposes multidimensional scaling (MDS) as a valuable statistical tool for geological data analysis. The solid line signifies the strongest correlation, while the dashed line represents the second strongest correlation. Through MDS analysis, both the Miaoling Formation and Kedao Group have a higher affinity with NE China (Fig. 15). Zircons from these formations exhibit similar Hf isotopic compositions consistent

https://doi.org/10.1017/S0016756824000359 Published online by Cambridge University Press

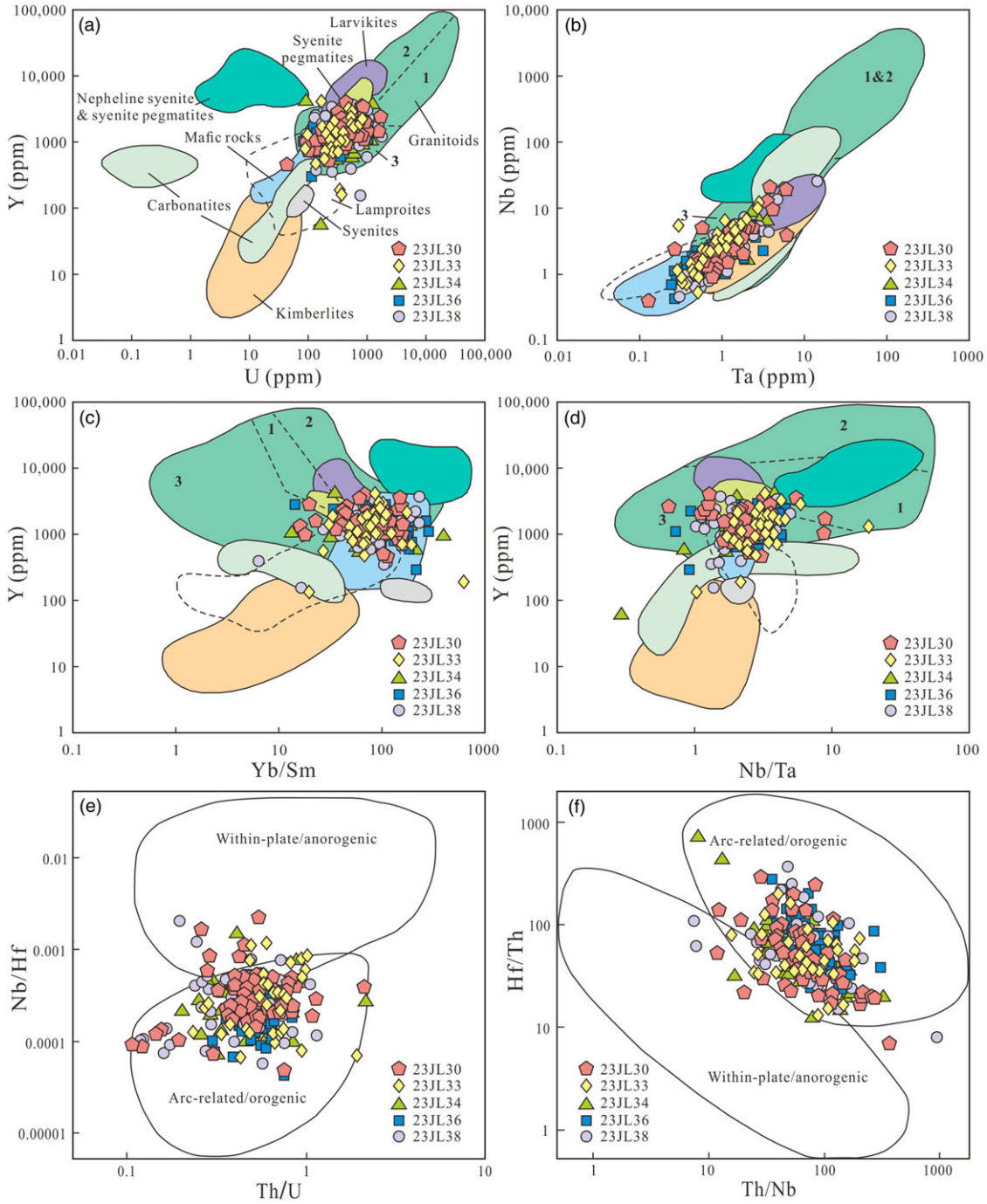

Figure 13. The fields of zircon compositions used as discriminants for different rock types (Belousova et al. 2002). (a) Zircon Y versus U, (b) Zircon Nb versus Ta, (c) Zircon Y versus Yb/Sm, (d) Zircon Y versus Nb/Ta, (e) Zircon Nb/Hf versus Th/U (Yang et al. 2012) and (f) Zircon Hf/Th versus Th/Nb (Yang et al. 2012).

with those from the CAOB, in line with the Hf isotope results of the magmatic rocks in the study area (Fig. 11; Shi et al. 2022; Lu et al. 2022; Shi et al. 2020), indicating a certain level of data reliability. The T_{DM2} did not provide evidence for an age of 2.5 billion years. Based on various evidence, we can confidently infer that the samples from both the Miaoling Formation and Kedao Group originated from NE China (Zhangguangcai Range and Jiamusi-Khanka block). Additionally, combined with the findings from other studies, we can boldly infer that the Permian to Triassic stratigraphic source areas in the eastern part of Jilin Province are more closely related to NE China (Sun et al. 2023; Du et al. 2019, 2021; Zhang et al. 2019), further supported by Hf isotope results from igneous rocks exposed in the surrounding area (Cao et al. 2013).

5. c. Tectonic setting

The oceanic subduction-continental collision system has become a research hotspot in recent years (Dai et al. 2018; Li et al. 2018a, b, 2019; Yu et al. 2019a, b, c; Zhang et al. 2019). The amalgamation of the NE China (XMOB) and the NCC along the SXCYS is widely believed to record the subduction and

https://doi.org/10.1017/S0016756824000359 Published online by Cambridge University Press

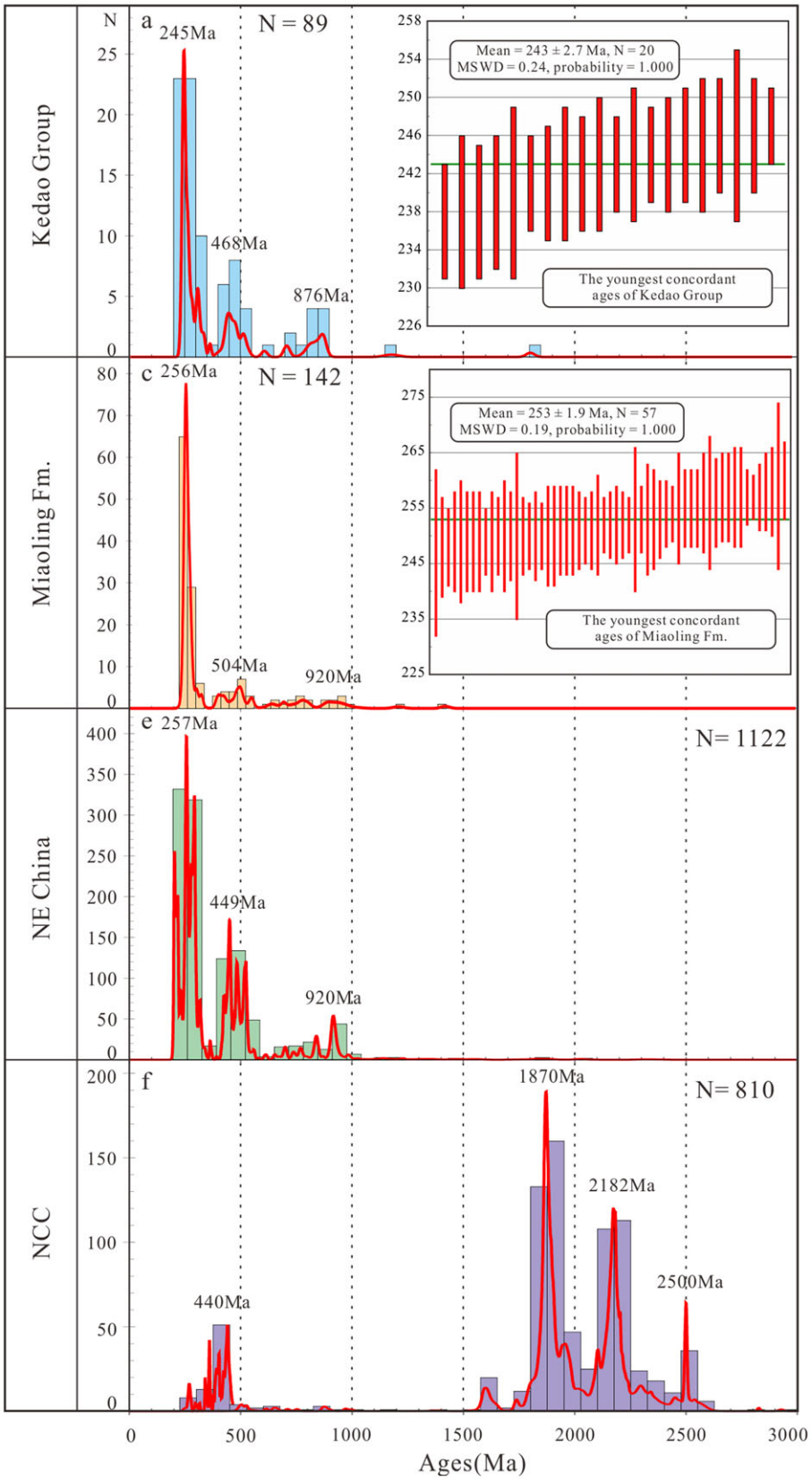

Figure 14. a-b. Age probability histograms of detrital zircons with concordant ages and the youngest weight mean age from the Kedao Group; c-d. Age probability histograms of detrital zircons with concordant ages and the youngest weight mean ages of the Miaoling Formation; e. The data originate from NE China (Zhangguangcai Range and Jiamusi-Khanka block; data from Du et al. 2016; Meng et al. 2011; Wang et al. 2012, 2015; Yu et al. 2013; Luan et al. 2017; Li, Y. et al. 2017; Long et al. 2019; Xue et al. 2023; Hua et al. 2019; Li, H.D. et al. 2022; Meng et al. 2017; Mou et al. 2023; Pu et al. 2015; Wen et al. 2017; Xiong et al. 2020; Zhang et al. 2021; Zhao et al. 2021; Zhao et al. 2023; Zhou et al.2013). f. The data originate from North China Craton; data from Liu et al. 2020, 2021; Chen et al. 2017, 2020; Fu et al. 2018; Li, G.S. et al. 2022; Liu et al. 2018; Pei et al. 2014; Peng et al. 2020; Peng & Wang, 2018; Shao et al. 2014; Yang et al. 2022; Zhang et al. 2015; Zhang et al. 2022; Zhang et al. 2013).

closure of the PAO (Sun et al. 2023), as indicated by the evidence from magmatic rocks, structural features and palaeontological data (Sun et al. 2004; Jia et al. 2004; Wu et al. 2007; Cao et al. 2013; Wang et al. 2015a, b; Li et al. 2017; Yang et al. 2017; Zhou et al. 2017; Gu et al. 2018; Du et al. 2019). In contrast to previous studies, we take a perspective of provenance analysis by concentrating on the sedimentary strata through petrology, geochronology and geochemistry in the Wangqing area along the

https://doi.org/10.1017/S0016756824000359 Published online by Cambridge University Press

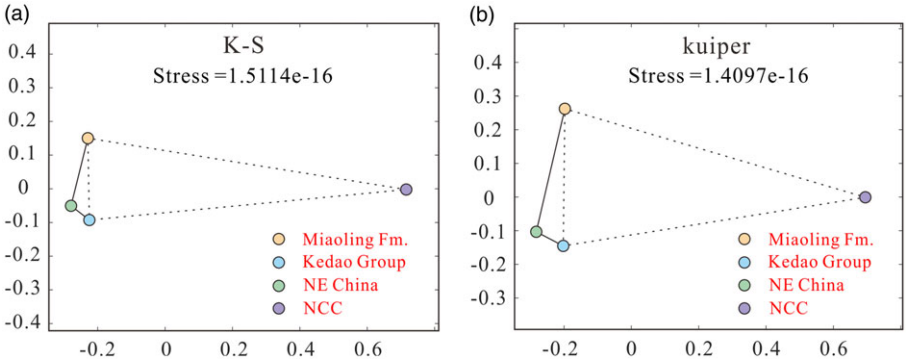

Figure 15. Multidimensional scaling (MDS) analysis results of Miaoling Formation, Kedao Group and surrounding potential source areas (NE China and North China Craton). a. After the standard K-S test. b. After the standard Kuiper test. (Vermeesch, 2013).

suture zone between the NCC and NE China (Fig. 1b). The Permian Miaoling Formation major consists of polycyclic sandstone, siltstone, silty mudstone and is the product of an arc-basin series. The Tanqian Formation, representing a muddy construction beneath the Carbonate Compensation Depth line of the abyssal plain, and the Shanguqi Formation, reflecting continental slope turbidites, together constitute the Kedao Group, which belongs to a deep-water slope-basinal sedimentary system (RGSR, 2007). The samples analyzed in this paper align well with previously established conditions. The Miaoling Formation and Kedao Group show distinct characteristics in various tectonic diagrams based on both major and trace elements (Figs. 9 and 10), with all geochemical data indicating their orogenic origin (Fig. 12e and f).

Zircon transport processes mainly influence the age distribution of detrital zircons in the strata, with peak age compositions effectively reflecting the tectonic environment of the sedimentary basin (Cawood et al. 2012). The convergent plate boundary is characterized by a large proportion of zircon ages close to the deposition age of the sediment, whereas sediments in collisional, extensional and intracratonic settings contain higher proportions of older ages reflecting the history of the underlying basement (Cawood et al. 2012). The majority of detrital zircons from the Miaoling Formation (70%) and Kedao Group (64%) have crystallization ages (CA) close to the depositional ages (DA) (CA-DA < 100 Ma), similar to the sedimentary facies of a convergent environment (Fig.16).

Verma & Armstrong-Altrin (2013) developed new discriminant-function-based major-element diagrams for classifying siliciclastic sediments from island or continental arc, continental rift and collision settings. The results of all sandstones indicate that the Wangqing area is still within the continental island arc (Fig. 17), reaffirming previous conclusions and indicating ongoing subduction of the PAO in this area during the Middle Triassic.

Recent studies on PAO evolution have documented considerable sedimentary evidence. Research on the southern part of the Great Xing'an Range and the Songliao Basin in NE China indicates that the PAO closed on the western side of the Changchun-Yanji suture zone in the Late Permian (He et al. 2023; Zhang et al. 2023). However, an alternative argument proposes a delayed closure of the eastern segment between the Middle Triassic and the Late Triassic (Zhang et al. 2019; Du et al, 2019). Igneous rocks in this region provide additional supporting evidence (Cao et al. 2013; Sun et al. 2023). Considering our new data with previously published data, Sun (2023) suggests that the volcanic interlayers of the Yangjiagou Formation formed in a syn-collisional setting,

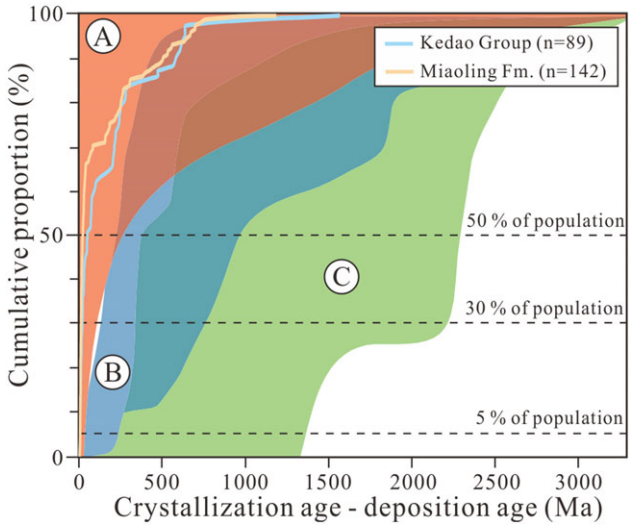

Figure 16. Summary plot of the general fields for convergent (A: red field), collisional (B: blue field), and extensional basins (C: greenfield). From the variations observed between the different fields, a model that predicts the tectonic setting of sedimentary packages of unknown origin is proposed based on differences between the crystallization and depositional ages (CA-DA) of the zircons.

implying a remnant ocean basin remained along the Changchun-Yanji suture zone during the Early Triassic. Furthermore, simulations of the crustal thickness in the central Jilin Province show that the crust gradually thickened from 280 Ma to 245 Ma, with the subduction of oceanic crust contributing to the continuous thickening of the continental crust (Guan et al. 2023). On a broader scale, Liang et al. (2019) summarize thermochronological data suggesting that significant strike-slip movement likely occurred in the Late Triassic, attributed to the eastward extrusion of the XMOB and far-field forces related to Late Triassic convergence following the final closure of the PAO.

The Miaoling Formation and the Kedao Group mainly originated from continental island arcs of NE China, including the Zhangguangcai Range and Jiamusi-Khanka block. During their sedimentation, a reduced remnant ocean basin remained in the Wangqing area, indicating that the PAO has not yet completed its closure until the early Middle Triassic (ca. 243 Ma; Fig. 18). Combining previous research suggests the final closure of the easternmost segment of the PAO likely occurred between the latest Middle Triassic and early Late Triassic in a scissor-like manner.

https://doi.org/10.1017/S0016756824000359 Published online by Cambridge University Press

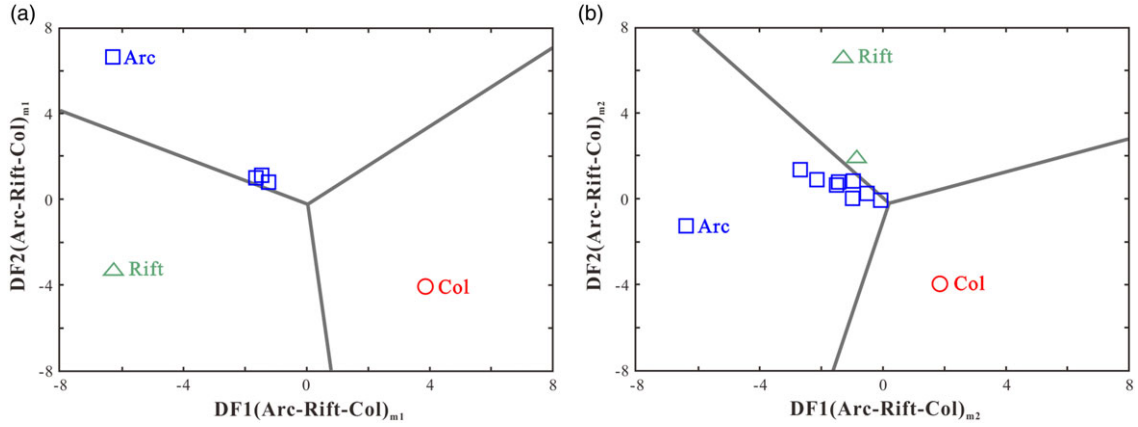

Figure 17. New discriminant-function multidimensional diagram for high-silica (a) and low-silica (b) clastic sediments from three tectonic settings (arc, continental rift and collision) (Verma & Armstrong-Altrin, 2013).

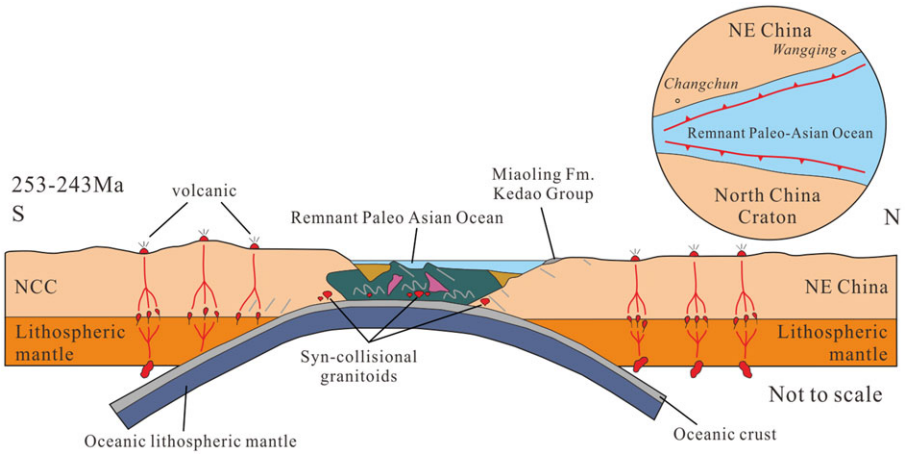

Figure 18. A sketch of the tectonic evolutionary pattern of the Paleo-Asian Ocean during 253–243Ma.

6. Conclusions

This study investigated the geochronology and geochemistry of the sandstones of the Miaoling Formation and the Kedao Group in the Wangqing area of NE China to determine their provenance and tectonic setting.

1. New LA–ICP–MS zircon U–Pb dating results show that the sedimentary rocks from the Miaoling Formation were deposited around 253 Ma, while the maximum depositional age of the Kedao Group is early Middle Triassic (ca. 243 Ma).

2. The Miaoling Formation and the Kedao Group are dominantly composed of Phanerozoic sediments originating from the NE China, suggesting that their parent rocks were likely felsic igneous rocks from an orogenic tectonic setting.

3. The provenance of these sedimentary strata has remained relatively consistent, implying that around 243 Ma, a small remnant ocean basin of PAO still existed in this area, and the continental blocks on the north and south sides had not yet completely converged. The final closure of the easternmost segment of the PAO likely occurred between the latest Middle Triassic and early Late Triassic in a scissor-like manner.

Supplementary material. The supplementary material for this article can be found at https://doi.org/10.1017/S0016756824000359

Acknowledgements. Special thanks to Qi Zheng from the School of Foreign Language Education, Jilin University, for the linguistic review that significantly improved the quality of the manuscript. We are grateful to the reviewers who helped improve the paper, and the editors for handling, editing and advising.

Financial support. This study was supported by the National Key R&D Program of China (Grant No. 2022YFF0800401-2), the National Natural Science Foundation of China (Grant No. 42130305) and Taishan Scholars (tstp20231214).

Competing interests. The authors declare that they have no known competing financial interests or personal relationships that could have appeared to influence the work reported in this paper.

References

Andersen T (2002) Correction of common lead in U–Pb analyses that do not report 204Pb. *Chemical Geology* **192**(1-2), 59–79. https://doi.org/10.1016/S0009-2541(02)00195-X

Belousova EA, Griffin WL, O'Reilly SY and Fisher NI (2002) Igneous zircon: trace element composition as an indicator of source rock type. *Contrib Mineral Petrol* **143**(5), 602–22. https://doi.org/10.1007/s00410-002-0364-7

BGMRJP (1997) *Stratigraphy (Lithostratigraphy) of Jilin Province*. China University of Geosciences Press, Wuhan. 1–324 (in Chinese).

Boynton WV (1984) Cosmochemistry of the rare earth elements: meteorite studies. *Developments in Geochemistry* **2**, 63–114. https://doi.org/10.1016/B978-0-444-42148-7.50008-3

Cao HH, Xu WL, Pei FP, Guo PY and Wang F (2012) Permian tectonic evolution of the eastern section of the northern margin of the North China Plate: constraints from zircon U-Pb geochronology and geochemistry of the

volcanic rocks. *Acta Petrologica Sinica* **28**(9), 2733–50 (in Chinese with English abstract).

Cao HH, Xu WL, Pei FP, Wang ZW, Wang F and Wang ZJ (2013) Zircon U-Pb geochronology and petrogenesis of the Late Paleozoic-Early Mesozoic intrusive rocks in the eastern segment of the northern margin of the North China Block. *Lithos* **170-171**, 191–207. https://doi.org/10.1016/j.lithos.2013.03.006

Cawood PA, Hawkesworth CJ and Dhuime B (2012) Detrital zircon record and tectonic setting. *Geology* **40**(10), 875–78. https://doi.org/10.1130/G32945.1

Chen B, Jahn BM and Tian W (2009) Evolution of the Solonker suture zone: constraints from zircon U-P ages, Hf isotopic ratios and whole-rock Nd-Sr isotope compositions of subduction- and collision-related magmas and forearc sediments. *Journal of Asian Earth Sciences* **34**(3), 245–57. https://doi.org/10.1016/j.jseaes.2008.05.007

Chen B, Jahn BM, Wilde S and Xu B (2000) Two contrasting Paleozoic magmatic belts in northern Inner Mongolia, China: petrogenesis and tectonic implications. *Tectonophysics* **328**, 157–82. https://doi.org/10.1016/S0040-1951(00)00182-7

Chen JS, Li WW, Shi Y, Li B, Zhao CQ and Zhang LD (2022) Evolution of the eastern segment of the northern margin of the North China Craton in the Triassic: Evidence from the geochronology and geochemistry of magmatic rocks in Kaiyuan area, North Liaoning. *Acta Petrologica Sinica* **38**(8), 2216–48 (in Chinese with English abstract).

Chen JS, Li WW, Xing DH, Yang ZZ, Tian DX, Zhang LD, Li B, Liu M and Yang F (2020) Zircon U-Pb Geochronology of Volcanic Rocks from Gaojiayu Formation, Liaohe Group, Liaoning Province and its geological significance. *Earth Science* **45**(11), 3934–49 (in Chinese with English abstract).

Chen JS, Xing DH, Liu M, Li B, Yang H, Tian DX, Yang F and Wang Y (2017) Zircon U-Pb chronology and geological significance of felsic volcanic rocks in the Liaohe Group from the Liaoyang area, Liaoning Province. *Acta Petrologica Sinica* **33**(9), 2792–810 (in Chinese with English abstract).

Condie K (1993) Chemical composition and evolution of the upper continental crust: Contrasting results from surface samples and shales. *Chemical Geology* **104**, 1–37. https://doi.org/10.1016/0009-2541(93)90140-E

Dai LM, Li SZ, Li ZH, Somerville I, Suo YH, Liu XC, Gerya T and Santosh M (2018) Dynamics of exhumation and deformation of HP-UHP orogens in double subduction-collision systems: Numerical modeling and implications for the Western Dabie Orogen. *Earth-Science Reviews* **182**, 68–84. https://doi.org/10.1016/j.earscirev.2018.05.005

Dickinson WR and Gehrels GE (2009) Use of U-Pb ages of detrital zircons to infer maximum depositional ages of strata: A test against a Colorado Plateau Mesozoic database. *Earth and Planetary Science Letters* **288**, 115–25. https://doi.org/10.1016/j.epsl.2009.09.013

Du QX, Han ZZ, Shen XL, Gao LH, Han M, Song ZG, Li JJ, Zhong WJ, Yan JL and Liu H (2016) Geochemistry and geochronology of Upper Permian-Upper Triassic volcanic rocks in eastern Jilin Province, NE China: implications for the tectonic evolution of the Palaeo-Asian Ocean. *International Geology Review* **59**(3), 368–90. https://doi.org/10.1080/00206814.2016.1266702

Du QX, Han ZZ, Shen XL, Han C, Song ZG, Gao LH, Han M and Zhong WJ (2019) Geochronology and geochemistry of Permo-Triassic sandstones in eastern Jilin Province (NE China): Implications for final closure of the Paleo-Asian Ocean. *Geoscience Frontiers* **10**, 683–704. https://doi.org/10.1016/j.gsf.2018.03.014

Du QX, Li GS, Han ZZ and Shen XL (2021) Reappraisal of ages of Triassic continental sedimentary successions in the Yanbian area (NE China): implications for the Triassic Angaran and Cathaysian floral recovery. *Journal of Asian Earth Sciences* **215**, 104811. https://doi.org/10.1016/j.jseaes.2021.104811

Eizenhöfer PR, Zhao GC, Zhang J and Sun M (2014) Final closure of the Paleo-Asian Ocean along the Solonker suture zone: constraints from geochronological and geochemical data of Permian volcanic and sedimentary rocks. *Tectonics* **33**, 441–63. https://doi.org/10.1002/2013TC003357

Fedo CM (2003) Detrital zircon analysis of the sedimentary record. *Reviews in Mineralogy and Geochemistry* **53**(1), 277–303. https://doi.org/10.2113/0530277

Fedo CM, Nesbitt HW and Young GM (1995) Unraveling the effects of potassium metasomatism in sedimentary rocks and paleosols, with implications for paleoweathering conditions and provenance. *Geology* **23**, 921–24. https://doi.org/10.1130/0091-7613(1995)023<0921:UTEOPM>2.3.CO;2

Feng GY, Liu S, Zhong H, Jia DC, Qi YQ, Wang T and Yang YH (2010) Geochemical characteristics and petrogenesis of late Paleozoic mafic rocks from Yumuchuan, Jilin Province. *Geochimica* **39**, 427–38 (in Chinese with English abstract). https://doi.org/10.19700/j.0379-1726.2010.05.003

Fu JY, Sun W, Wang Y, Zhong H, Na FC, Yang F, Zhang GY and Yu HB (2018) Zircon U-Pb chronology of the Toudaogou Mafic-Ultramafic Rocks from Yongji, Jilin Province, and its geological implications. *Acta Geologica Sinica* **92**(09), 1859–72 (in Chinese with English abstract).

Ge WC, Wu FY, Zhou CY and Zhang JH (2005) Zircon U-Pb ages and its significance of the Mesozoic granites in the Wulanhaote region, central Da Hinggan Mountaim. *Acta Petrologica Sinica* **21**, 749–62 (in Chinese with English abstract).

Gu CC, Zhu G, Li YJ, Su N, Xiao SY, Zhang S and Li C (2018) Timing of deformation and location of the eastern Liaoyuan Terrane, NE China: Constraints on the final closure time of the Paleo-Asian Ocean. *Gondwana Research* **60**, 194–212. https://doi.org/10.1016/j.gr.2018.04.012

Guan QB, Liu ZH, Liu YJ, Li SZ, Wang SJ, Chen ZX and Zhang C (2022) A tectonic transition from closure of the Paleo-Asian ocean to subduction of the Paleo-Pacific Plate: Insights from early Mesozoic igneous rocks in eastern Jilin Province, NE China. *Gondwana Research* **102**, 332–53. https://doi.org/10.1016/j.gr.2020.05.001

Guan ZC, Pei FP, Wei JY and Li PY (2023) U-Pb-Hf Isotopic Compositions of Detrital Zircons from the Wanbaoyan Formation in the Dunhua Area of Jilin: Constraints on Regional Tectonic Evolution. *Journal of Jilin University (Earth Science Edition)* **54**(04), 1264–79 (in Chinese with English abstract). https://doi.org/10.13278/j.cnki.jjuese.20230081

Guo F, Li H, Fan W, Li J, Zhao L and Huang M (2016) Variable sediment flux in generation of Permian subductionrelated mafic intrusions from the Yanbian region, NE China. *Lithos* **261**, 195–215. https://doi.org/10.1016/j.lithos.2015.11.030

Han J, Zhou JB, Wang B and Cao JL (2015) The final collision of the CAOB: constraint from the zircon U-Pb dating of the Linxi Formation, Inner Mongolia. *Geoscience Frontiers* **6**(2), 211–25. https://doi.org/10.1016/j.gsf.2014.06.003

Han ZZ, Li JJ, Song ZG, Liu GY, Zhong WJ, Gao LH and Du QX (2020) Geochemistry and zircon U-Pb-Hf isotopes of metamorphic rocks from the Kaiyuan and Hulan Tectonic Melanges, NE China: Implications for the tectonic evolution of the Paleo-Asian and Mudanjiang Oceans. *Minerals* **10**(9), 836. https://doi.org/10.3390/min10090836

Han ZZ, Li JJ, Zhu CL, Zhong WJ and Song ZG (2021) The late Triassic Molasse deposits in Central Jilin Province, NE China: constraints on the Paleo-Asian ocean Closure. *Minerals* **11**, 223. https://doi.org/10.3390/min11020223

Han ZZ, Zhong WJ, Song ZG, Han C, Han M, Gao LH, Du QX, Li JJ, Yan JL and Liu H (2019) Geochronology and geochemistry of metasedimentary rocks from the Dongnancha Formation in the Huadian area, central Jilin Province, Northeast (NE) China: implications for the tectonic evolution of the eastern segment of the Paleo-Asian Ocean. *Geochemistry* **79**(1), 94–112. https://doi.org/10.1016/j.geoch.2018.12.002

He D, Fang H, Zhang P, Pei F, Ming C, He M and Zhang X (2023) Geochemical characteristics of the Middle-Late Permian sedimentary rocks in the southern Great Xing'an Range, NE China, and their constraints on the closure time of the Paleo Asian Ocean (Eastern Segment). *Sedimentary Geology* **450**, 106375. https://doi.org/10.1016/j.sedgeo.2023.106375

Herron MM (1988) Geochemical classification of terrigenous sands and shales from core or log data. *Journal of Sedimentary Petrology* **58**, 820–29. https://doi.org/10.1306/212F8E77-2B24-11D7-8648000102C1865D

Hong DW, Huang HZ, Xiao YJ, Xu HM and Jin MY (1995) Permian alkaline granites in central Inner Mongolia and their geodynamic significance. *Acta Geologica Sinica (English Edition)* **8**, 27–39. https://doi.org/10.1111/j.1755-6724.1995.mp8001003.x

Hua YC, Zhang SM, Zhang SF, Xiao ZX and Zhang SQ (2019) U-Pb zircon age and geochemical characteristics of Early Paleozoic granites in the

Baoqing area, Heilongjiang Province. *Geological Bulletin of China* **38**(7), 1228–39 (in Chinese with English abstract).

Huang JX, Zhao ZD, Zhang HF, Hou QY, Chen YL, Zhang BR and Depaolo DJ (2006) Elemental and Sr-Nd-Pb isotopic geochemistry of the Wenduermiao and BayanaobaoJiaoqier ophiolites, Inner Mongolia: constraints for the characteristics of the mantle domain of eastern Paleo-Asian Ocean. *Acta Petrologica Sinica* **22**, 2889–900 (in Chinese with English abstract).

Jia DC, Hu RZ, Lu Y and Qiu XL (2004) Collision belt between the Khanka block and the north China block in the Yanbian region, Northeast China. *Journal of Asian Earth Sciences* **23**, 211–19. https://doi.org/10.1016/S1367-9120(03)00123-8

Jian P, Liu DY, Kröner A, Windley BF, Shi YR, Zhang W, Zhang FQ, Miao LC, Zhang LQ and Tomurhuu D (2010) Evolution of a Permian intraoceanic arc-trench system in the Solonker suture zone, Central Asian Orogenic Belt, China and Mongolia. *Lithos* **18**, 169–90. https://doi.org/10.1016/j.lithos.2010.04.014

Khain EV, Bibikova EV, Kroneĭ A, Zhuravlev DZ, Sklyarov EV, Fedotova AA and Kravchenko-Berezhnoy IR (2002) The most ancient ophiolite of the Central Asian fold belt: U-Pb and Pb-Pb zircon ages for the Dunzhugur Complex, Eastern Sayan, Siberia, and geodynamic implications. *Earth and Planetary Science Letters* **199**(3), 311–25. https://doi.org/10.1016/S0012-821X(02)00587-3

Li GS, Du QX, Han ZZ and Shen XL (2022) Geochronology, Petrogenesis and Tectonic Significance of Intermediate-Acid Magmatic Rocks in Yanbian Area, Eastern Jilin. *Journal of Jilin University (Earth Science Edition)* **52**(4), 1174–202 (in Chinese with English abstract). https://doi.org/10.13278/j.cnki.jjuese.20210119

Li HD, Zhou JB, Li GY, Wang B, Chen Z and Wang HY (2022) Nature and evolution of the South Tianshan Mountains-Beishan Mountains-Solonker-Changchun Suture. *Geological Review* **68**(03), 797–816 (in Chinese with English abstract). https://doi.org/10.16509/j.georeview.2022.02.061

Li JY (1998) Some new ideas on tectonics of NE China and its neighboring area. *Geological Review* **44**, 339–47 (in Chinese with English abstract). https://doi.org/10.16509/j.georeview.1998.04.002

Li JY (2006) Permian geodynamic setting of Northeast China and adjacent regions: closure of the Paleo-Asian Ocean and subduction of the Paleo-Pacific Plate. *Journal of Asian Earth Sciences* **26**, 207–24. https://doi.org/10.1016/j.jseaes.2005.09.001

Li SK, Liu JL, Zhou YH and Liu EQ (2020) Late Permian tectonic evolution at the eastern margin of the Songnen-Zhangguangcai Range Massif, NE China: evidence from geochronology and geochemistry of the Deyu granitoids. *Acta Geologica Sinica* **94**, 450–66 (in Chinese with English abstract). https://doi.org/10.19762/j.cnki.dizhixuebao.2020151

Li SZ, Suo YH, Li XY, Liu B, Dai LM, Wang GZ, Zhou J, Li Y, Liu YM, Cao XZ, Somerville I, Mu DL, Zhao SJ, Liu JP, Meng F, Zhen LB, Zhao LT, Zhu JJ, Yu SY, Liu YJ and Zhang GW (2018a) Microplate tectonics: new insights from micro-blocks in the global oceans, continental margins and deep mantle. *EarthScience Reviews* **185**, 1029–64. https://doi.org/10.1016/j.earscirev.2018.09.005

Li SZ, Suo YH, Li XY, Zhou J, Santosh M, Wang PC, Wang GZ, Guo LL, Yu SY, Lan HY, Dai LM, Zhou ZZ, Gao XZ, Zhu JJ, Liu B, Jiang SH, Wang G and Zhang GW (2019) Mesozoic tectono-magmatic response in the East Asian ocean-continent connection zone to subduction of the Paleo-Pacific Plate. *Earth-Science Reviews* **192**, 91137. https://doi.org/10.1016/j.earscirev.2019.03.003

Li SZ and Zhao GC (2007) SHRIMP U-Pb zircon geochronology of the Liaoji granitoids: Constraints on the evolution of the Paleoproterozoic Jiao-Liao-Ji belt in the eastern block of the North China Craton. *Precambrian Research* **158**(1-2), 1–16. https://doi.org/10.1016/j.precamres.2007.04.001

Li SZ, Zhao SJ, Liu X, Cao HH, Yu S, Li XY, Somerville I, Yu SY and Suo YH (2018b) Closure of the Proto-Tethys Ocean and Early Paleozoic amalgamation of microcontinental blocks in East Asia. *Earth-Science Reviews* **186**, 37–75. https://doi.org/10.1016/j.earscirev.2017.01.011

Li Y, Xu WL, Wang F, Tang J, Sun CY and Wang ZJ (2017) Early-Middle Ordovician volcanism along the eastern margin of the Xing'an Massif, Northeast China: constraints on the suture location between the Xing'an and Songnen-Zhangguangcai Range massifs. *International Geology Review* **60**(16), 2046–62. https://doi.org/10.1080/00206814.2017.1402378

Li YL, Brouwer FM, Xiao WJ, Wang KL, Lee YH, Luo BJ, Su YP and Zheng JP (2017) Subduction-related metasomatic mantle source in the eastern central Asian orogenic belt: evidence from amphibolites in the Xilingol complex, inner Mongolia, China. *Gondwana Research* **43**, 193–212. https://doi.org/10.1016/j.gr.2015.11.015

Li YL, Zhou HW, Brouwer FM, Xiao WJ, Wijbrans JR, Zhao JH, Zhong ZQ and Liu HF (2014) Nature and timing of the Solonker suture of the Central Asian Orogenic Belt: insights from geochronology and geochemistry of basic intrusions in the Xilin Gol Complex, Inner Mongolia, China. *International Journal of Earth Sciences* **103**, 41–60. https://doi.org/10.1007/s00531-013-0931-3

Liang CY, Liu YJ, Zheng CQ, Li WM, Franz NEUBAUER and Zhang Q (2019) Macro-and Microstructural, Textural Fabrics and Deformation Mechanism of Calcite Mylonites from Xar Moron-Changchun Dextral Shear Zone, Northeast China. *Acta Geologica Sinica (English Edition)* **93**(5), 1477–99. https://doi.org/10.1111/1755-6724.14357

Lin SZ, Zhu G, Yan LJ, Song LH and Liu B (2013) Structural and chronological constraints on a Late Paleozoic shortening event in the Yanshan Tectonic Belt. *Chinese Science Bulletin* **58**(32), 3922–36. https://doi.org/10.1007/s11434-013-5926-8

Liu J, Liu ZH, Zhao C, Wang CJ, Guan QB, Dou SY and Song S (2017) Geochemistry and U-Pb detrital zircon ages of late Permian to Early Triassic metamorphic rocks from northern Liaoning, North China: evidence for the timing of final closure of the Paleo-Asian Ocean. *Journal of Asian Earth Sciences* **145**, 460–74. https://doi.org/10.1016/j.jseaes.2017.06.026

Liu J, Zhang J, Liu ZH, Yin CQ, Xu ZY, Cheng CQ, Zhao C and Wang X (2021) Late Paleoproterozoic crustal thickening of the Jiao-Liao-Ji belt, North China Craton: insights from ca.1.95-1.88 Ga syn-collisional adakitic granites. *Precambrian Research* **355**, 106120. https://doi.org/10.1016/j.precamres.2021.106120

Liu J, Zhang J, Yin C, Cheng C, Liu X, Zhao C, Chen Y and Wang X (2020) Synchronous A-type and adakitic granitic magmatism at ca. 2.2 Ga in the Jiao-Liao-Ji belt, North China Craton: Implications for rifting triggered by lithospheric delamination. *Precambrian Research* **342**, 105629. https://doi.org/10.1016/j.precamres.2020.105629

Liu S, Hu RZ, Gao S, Feng CX, Feng GY, Coulson IM, Li C, Wang T and Qi YQ (2010) Zircon U-Pb age and Sr-Nd-Hf isotope geochemistry of Permian granodiorite and associated gabbro in the Songliao Block, NE China and implications for growth of juvenile crust. *Lithos* **114**, 423436. https://doi.org/10.1016/j.lithos.2009.10.009

Liu WB, Peng YB, Zhao C, Cui YS, Yang CH and Wen C (2018) LA-ICP-MS Zircon U-Pb dating and geochemistry of wolongquan intrusion in gaizhou, southern liaoning province. *Geology and Resources* **27**(06), 531–39 (in Chinese with English abstract). https://doi.org/10.13686/j.cnki.dzyzy.2018.06.005

Liu YJ, Li WM, Feng ZQ, Wen QB, Neubauer F and Liang CY (2017) A review of the paleozoic tectonics in the eastern part of central Asian orogenic belt. *Gondwana Research* **43**, 123–48. https://doi.org/10.1016/j.gr.2016.03.013

Long XY, Xu WL, Guo P, Sun CY and Luan JP (2019) Was Permian magmatism in the eastern Songnen and western Jiamusi massifs, NE China, related to the subduction of the Mudanjiang oceanic plate? *Geological Journal* **55**(3), 1781–807. https://doi.org/10.1002/gj.3577

Lu SY, Ren YS, Hou HN, Li JM, Hao YJ and Shang QQ (2022) Petrogenesis, tectonic setting, and metallogenic significance of the Middle Permian volcanic rock system of the Miaoling Formation, Yanbian area, NE China: Constraints from geochronology, geochemistry, and Sr-Nd-Hf isotopes. *Geochemistry* **82**, 125902. https://doi.org/10.1016/j.chemer.2022.125902

Luan JP, Xu WL, Wang F, Wang ZW and Guo P (2017) Age and geochemistry of the Neoproterozoic granitoids in the Songnen-Zhangguangcai Range Massif, NE China: petrogenesis and tectonic implications. *Journal of Asian Earth Sciences* **148**, 265–76. https://doi.org/10.1016/j.jseaes.2017.09.011

Ludwig KR (2003) Isoplot 3.09-A Geochronological Toolkit for Microsoft Excel. Berkeley Geochronology Center Special Publication, 1–4.

McDonough WF and Sun S-S (1995) Composition of the Earth. *Chemical Geology* **120**: 223–53.

https://doi.org/10.1017/S0016756824000359 Published online by Cambridge University Press

Meng E, Xu WL, Pei FP, Yang DB, Wang F and Zhang XZ (2011) Permian bimodal volcanism in the Zhangguangcai Range of eastern Heilongjiang Province, NE China: zircon U-Pb-Hf isotopes and geochemical evidence. *Journal of Asian Earth Sciences* **41**(2), 119–32. https://doi.org/10.1016/j.jseaes.2011.01.005

Meng J, Liu XY, Liang YH, Qin Y, Ju G and Li BX (2017) U-Pb Dating and Trace Elements Composition of Tadong Group from Jilin Province and Their Geological Implications. *Earth Science* **42**(4), 502–10 (in Chinese with English abstract).

Mi K, Liu Z, Li C, Liu R, Wang J and Peng R (2017) Origin of the Badaguan porphyry Cu-Mo deposit, Inner Mongolia, northeast China: Constraints from geology, isotope geochemistry and geochronology. *Ore Geology Reviews* **81**, 154–72. https://doi.org/10.1016/j.oregeorev.2016.09.029

Mou RT, Pei FP, Shi YQ and Wei JY (2023) Genesis of Early Permian Volcanic Rocks in Yitong Area, Central Jilin Province: Constraints from Zircon U-Pb Geochronology and Whole-Rock Geochemistry. *Journal of Jilin University (Earth Science Edition)* **53**(4), 1117–31 (in Chinese with English abstract). https://doi.org/10.13278/j.cnki.jjuese.20220114

Nesbitt HW and Young GM (1984) Prediction of some weathering trends of plutonic and volcanic rocks based on thermodynamic and kinetic considerations. *Geochimica et Cosmochimica Acta* **48** (7), 1523–34. https://doi.org/10.1016/0016-7037(84)90408-3

Pei FP, Wang ZW, Cao HH, Xu WL and Wang F (2014) Petrogenesis of the Early Paleozoic tonalite in the central Jilin Province: Evidence from zircon U-Pb chronology and geochemistry. *Acta Petrologica Sinica* **30**(7), 2009–19.

Pei FP, Zhang Y, Wang ZW, Cao HH, Xu WL, Wang ZJ, Wang F and Yang C (2016) Early-Middle Paleozoic subduction-collision history of the southeastern Central Asian Orogenic Belt: Evidence from igneous and metasedimentary rocks of central Jilin Province, NE China. *Lithos* **261**, 164–80. https://doi.org/10.1016/j.lithos.2015.12.010

Peng YB, Liu WB, Zhao J, Zhao J, Cui YS, Yang CH, Zhao C and Wen C (2020) Geochemical Characteristics, LA-ICP-MS Zircon U-Pb Dating and Geological Significance of Southern Liaoning Province Pluton: A Case Study of Triassic Pluton in Gaizhou Wanfu-Xiuyuan Longtan Area. *Journal of Jilin University (Earth Science Edition)* **50**(6), 1737–51 (in Chinese with English abstract). https://doi.org/10.13278/j.cnki.jjuese.20200013

Peng YB and Wang ED (2018) LA-ICP-MS zircon U-Pb dating and geochemical characteristics of Paleoproterozoic rock mass in Liangtun-Kuangdonggou area of South Liaoning province. *Science Technology and Engineering* **18**(20), 41–50 (in Chinese with English abstract).

Peng YJ, Qi CD, Zhou XD, Lu XB, Dong HC and Li Z (2012) Transition from PaleoAsian ocean domain to circum -pacific Ocean domain for the Ji-Hei composite orogenic belt: time mark and relationship to global tectonics. *Geology and Resources* **21**, 261–65 (in Chinese with English abstract). https://doi.org/10.13686/j.cnki.dzyzy.2012.03.012

Pettijohn FJ, Potter PE and Siever R (1972) Sand and Sandstone. *New York: Springer-Verlag* 1–618.

Pu JB, Zhang XZ, Guo Y, Zeng Z, Fu QL, Zhang HT and Liu Y (2015) Geological implications of Permian Fangshan granitic rocks in eastern Jiamusi Massif: evidences from U-Pb chronology and geochemistry. *Global Geology* **34**(04), 903–13 (in Chinese with English abstract).

Regional Geological Survey Report (RGSR) (2007) China Geological Survey (CGS), K52C001003 (in China).

Ren Q, Zhang SH, Sukhbaatar T, Hou MC, Wu HC, Yang TS, Li HY and Chen AQ (2023) Timing the Hegenshan suture in the Central Asian Orogenic Belt: New Paleomagnetic and Geochronological constraints from Southeastern Mongolia. *Geophysical Research Letters* **50**(20), e2023GL104881. https://doi.org/10.1029/2023GL104881

Rudnick RL and Gao S (2014) Composition of the Continental Crust. Elsevier, 1–64. https://doi.org/10.1016/B978-0-08-095975-7.00301-6

Rudnick RL, Gao S, Ling WL, Liu YS and McDonough WF (2004) Petrology and geochemistry of spinel peridotite xenoliths from Hannuoba and Qixia, North China Craton. *Lithos* **77**, 609–37. https://doi.org/10.1016/j.lithos.2004.03.033

Santosh M and Somerville ID (2013) Tectonic evolution of the North China Craton: introduction. *Geological Journal* **48**, 403–05. https://doi.org/10.1002/gj.2518

Sengör AMC, Natal'in BA and Burtman VS (1993) Evolution of the Altaid tectonic collage and Palaeozoic crustal growth in Eurasia. *Nature* **364**, 299–307.

Shao JB, Li JG, Wang HT, Chen DY and Ren Q (2014) Geological characteristics and zircon U-Pb age of the Wudaoyangcha Neoarchaean vanadic titanomagnetite deposit in Baishan,Jilin Province. *Geology In China* **41**(02), 463–83 (in Chinese with English abstract).

Shen XL, Du QX, Han ZZ, Song ZG, Han C, Zhong WJ and Ren X (2019) Constraints of zircon U-Pb-Hf isotopes from Late Permian-Middle Triassic flora-bearing strata in the Yanbian area (NE China) on a scissor-like closure model of the Paleo-Asian Ocean. *Journal of Asian Earth Sciences* **183**, 103964. https://doi.org/10.1016/j.jseaes.2019.103964

Shi CL, Ding XZ, Liu YX and Zhou XD (2020) Detrital zircon U-Pb dating and Hf isotope study of late Palaeozoic sedimentary rocks in central-eastern Jilin Province, NE China: Constraints for tectonic evolution of the eastern segment of the Paleo-Asian Ocean. *Geological Journal* **55**(4), 2717–37. https://doi.org/10.1002/gj.3525

Shi CL, Ding XZ, Zhou XD, Nie LJ and Zhang JB (2022) Geochronology, Geochemistry and Sr-Nd-Hf Isotopes of Early-Middle Triassic Adakitic Plutons in Central-eastern Jilin Province, NE China: Constraints on the non-synchronous Closure of Paleo-Asian Ocean. *Acta Geologica Sinica* (Eng) **96**, 1615–30. https://doi.org/10.1111/1755-6724.14906

Shi YR, Liu DY, Miao LC, Zhang FQ, Jian P, Zhang W, Hou KJ and Xu JY (2010) Devonian A-type granitic magmatism on the northern margin of the North China Craton: SHRIMP U-Pb zircon dating and Hf-isotopes of the Hongshan granite at Chifeng, Inner Mongolia, China. *Gondwana Research* **17**(4), 632–41. https://doi.org/10.1016/j.gr.2009.11.011

Sircombe KN (1999) Tracing provenance through the isotope ages of littoral and sedimentary detrital zircon, eastern Australia. *Sedimentary Geology* **124**, 47–67. https://doi.org/10.1016/S0037-0738(98)00120-1

Sircombe KN (2004) AgeDisplay: an EXCEL workbook to evaluate and display univariate geochronological data using binned frequency histograms and probability density distributions. *Computational Geosciences* **30**, 21–31. https://doi.org/10.1016/j.cageo.2003.09.006

Sláma J, Košler J, Condon DJ, Crowley JL, Gerdes A, Hanchar JM, Horstwood MSA, Morris GA, Nasdala L, Norberg N, Schaltegger U, Schoene B, Tubrett MN and Whitehouse MJ (2008) Plešovice zircon — A new natural reference material for U-Pb and Hf isotopic microanalysis. *Chemical Geology* **249**, 1–35. https://doi.org/10.1016/j.chemgeo.2007.11.005

Song ZG, Han ZZ, Gao LH, Geng HY, Li XP, Meng FX, Han M, Zhong WJ, Li JJ, Du QX, Yan JL and Liu H (2018) Permo-Triassic evolution of the southern margin of the Central Asian Orogenic Belt revisited: insights from late Permian igneous suite in the Daheishan Horst, NE China. *Gondwana Research* **56**, 23–50. https://doi.org/10.1016/j.gr.2017.12.005

Sun DY, Gou J and Wang TH (2013) Geochronological and geochemical constraints on the Erguna Massif Basement, NE China-subduction history of the Mongol-Okhotsk Oceanic Crust. *International Geology Review* **55**(14), 1801–16. https://doi.org/10.1080/00206814.2013.804664

Sun DY, Wu FY, Zhang YB and Gao S (2004) The final closing time of the west Lamulun River-Changchun-Yanji plate suture zone: evidence from the Dayushan granitic pluton of Jilin. *Journal of Jilin University* (Earth Science Edition) **34** (2), 174–81 (in Chinese with English abstract). https://doi.org/10.13278/j.cnki.jjuese.2004.02.003

Sun HY (1988) Research progress of Permian in Yanbian area, Jilin Province. *Journal of Stratigraphy* **12** (3), 202–10 (in Chinese). https://doi.org/10.19839/j.cnki.dcxzz.1988.03.005

Sun SN, Han ZZ and Song ZG (2022) Age, provenance and geological significance of (meta)-sedimentary rocks in the Yitong-Gongzhuling area, NE China: constraints from zircon U-Pb geochronology. *Journal of Mineralogical and Petrological Sciences* **117**(1), e211224. https://doi.org/10.2465/jmps.211224

Sun SN, Song ZG, Han ZZ, Ji ZG, Zhou JG, Qin RY, Li JJ and Zhong WJ (2023) Relict basin closure of the Paleo-Asian Ocean: New insights from geochronological and geochemical analysis of the Yangjiagou Formation, NE China. *Lithos* **442**, 107074. https://doi.org/10.1016/j.lithos.2023.107074

Tang J, Xu WL, Wang F, Wang W, Xu MJ and Zhang YH (2013) Geochronology and geochemistry of Neoproterozoic magmatism in the Erguna Massif, NE China: Petrogenesis and implications for the breakup of

the Rodinia supercontinent. *Precambrian Research* **224**, 597–611. https://doi.org/10.1016/j.precamres.2012.10.019

Tang KD (1989) On tectonic development of the fold belts in the North margin of Sino-Korean Platform. *Geoscience* **3**, 195–204 (in Chinese with English abstract).

Verma SP and Armstrong-Altrin JS (2013) New multi-dimensional diagrams for tectonic discrimination of siliciclastic sediments and their application to Precambrian basins. *Chemical Geology* **355**, 117–33. https://doi.org/10.1016/j.chemgeo.2013.07.014

Vermeesch P (2013) Multi-sample comparison of detrital age distributions. *Chemical Geology* **341**, 140–46. https://doi.org/10.1016/j.chemgeo.2013.01.010

Wang F, Xu WL, Meng E, Cao HH and Gao FH (2012) Early Paleozoic amalgamation of the Songnen-Zhangguangcai Range and Jiamusi massifs in the eastern segment of the Central Asian Orogenic Belt: geochronological and geochemical evidence from granitoids and rhyolites. *Journal of Asian Earth Sciences* **49**, 234–48. https://doi.org/10.1016/j.jseaes.2011.09.022

Wang F, Xu WL, Xu YG, Gao FH and Ge WC (2015) Late Triassic bimodal igneous rocks in eastern Heilongjiang Province, NE China: implications for the initiation of subduction of the Paleo-Pacific Plate beneath Eurasia. *Journal of Asian Earth Sciences* **97**, 406–23. https://doi.org/10.1016/j.jseaes.2014.05.025

Wang ZJ, Xu WL, Pei FP, Wang ZW and Li Y (2015a) Geochronology and provenance of detrital zircons from late Palaeozoic strata of central Jilin Province, Northeast China: implications for the tectonic evolution of the eastern Central Asian Orogenic Belt. *International Geology Review* **57**(2), 211–28. https://doi.org/10.1080/00206814.2014.1002118

Wang ZJ, Xu WL, Pei FP, Wang ZW, Li Y and Cao HH (2015b) Geochronology and geochemistry of middle Permian-Middle Triassic intrusive rocks from central-eastern Jilin Province, NE China: Constraints on the tectonic evolution of the eastern segment of the Paleo-Asian Ocean. *Lithos* **238**, 13–25. https://doi.org/10.1016/j.lithos.2015.09.019

Wen QB, Liu YJ, Gao F, Xu M, Li WM, Feng ZQ, Zhou JP and Liang CY (2017) Thermochronological evidence for multi-phase uplifting and exhumation history of the Jiamusi uplift in eastern Heilongjiang, China. *Acta Petrologica Sinica* **33**(6), 1789–804 (in Chinese with English abstract).

Wiedenbeck M, Alle P, Corfu F, Griffin WL, Meier M, Oberli F, Vonquadt A, Roddick JC and Spiegel W (1995) Three Natural Zircon Standards for U-Th-Pb, Lu-Hf, Trace Element and REE Analyses. *Geostandards and Geoanalytical Research* **19**, 1–23. https://doi.org/10.1111/j.1751-908X.1995.tb00147.x

Wilde SA (2015) Final amalgamation of the Central Asian Orogenic Belt in NE China: Paleo-Asian Ocean closure versus Paleo-Pacific plate subduction - a review of the evidence. *Tectonophysics* **662**, 345–62. https://doi.org/10.1016/j.tecto.2015.05.006

Windley BF, Alexeiev D, Xiao WJ, Kröner A and Badarch G (2007) Tectonic models for accretion of the Central Asian Orogenic belt. *Journal of the Geological Society* **164**, 31–47. https://doi.org/10.1144/0016-76492006-022

Wu DD and Li M (2022) Whole-rock Sr-Nd-Li isotopic characteristics and genesis of the Triassic Jiefangyingzi pluton on the southeast margin of the Central Asian Orogenic Belt. *Earth Science* **47**(09), 3301–15 (in Chinese with English abstract).

Wu FY, Sun DY, Ge WC, Zhang YB, Grant ML, Wilde SA and Jahn BM (2011) Geochronology of the Phanerozoic granitoids in northeastern China. *Journal of Asian Earth Sciences* **41**, 1–30. https://doi.org/10.1016/j.jseaes.2010.11.014

Wu FY, Zhao GC, Sun DY, Wilde SA and Yang JH (2007) The Hulan Group: its role in the evolution of the Central Asian Orogenic Belt of NE China. *Journal of Asian Earth Sciences* **30**, 542–56. https://doi.org/10.1016/j.jseaes.2007.01.003

Wu YB and Zheng YF (2004) Genesis of zircon and its constraints on interpretation of U-Pb age. *Chinese Science Bulletin* **49**, 1554–69. https://doi.org/10.1360/04wd0130

Xiao WJ, Windley BF, Hao J and Zhai MG (2003) Accretion leading to collision and the Permian Solonker suture, Inner Mongolia, China: termination of the central Asian orogenic belt. *Tectonics* **22**(6), 1069. https://doi.org/10.1029/2002TC001484

Xiao WJ, Windley BF, Sun S, Li JL, Huang BC, Han CM, Yuan C, Sun M and Chen HL (2015) A tale of amalgamation of three Permo-Triassic Collage Systems in Central Asia: oroclines, sutures, and terminal accretion. *Annual Review of Earth and Planetary Sciences* **43**, 477–507. https://doi.org/10.1146/annurev-earth-060614-105254

Xiong S, Xu WL, Wang F and Ge WC (2020) Formation age and provenance of the Iman Group in the Khanka Massif: Evidence from U-Pb geochronology of detrital and magmatic zircons. *Acta Petrologica Sinica* **36**(3), 741–58 (in Chinese with English abstract).

Xu B and Chen B (1997) Framework and evolution of the middle Paleozoic orogenic belt between Siberian and North China plate in northern Inner Mongolia. *Science in China* (Earth Sciences) **40**, 463–69. https://doi.org/10.1007/BF02877610

Xu B, Zhao P, Bao QZ, Zhou YH,Wang YY and Luo ZW (2014) Preliminary study on the pre-Mesozoic tectonic unit division of the Xing-Meng Orogenic Belt (XMOB). *Acta Petrologica Sinica* **30**(7), 1841–57 (in Chinese with English abstract).

Xu B, Zhao P, Wang Y, Liao W, Luo Z, Bao Q and Zhou Y (2015) The pre-Devonian tectonic framework of Xing'an-Mongolia orogenic belt (XMOB) in North China. *Journal of Asian Earth Sciences* **97**, 183–96. https://doi.org/10.1016/j.jseaes.2014.07.020

Xu WL, Ji WQ, Pei FP, Meng E, Yu Y, Yang DB and Zhang XZ (2009) Triassic volcanism in eastern Heilongjiang and Jilin provinces, NE China: chronology, geochemistry, and tectonic implications. *Journal of Asian Earth Sciences* **34**, 392–402. https://doi.org/10.1016/j.jseaes.2008.07.001

Xue YT, Tang J, Xu WL, Luan JP, Long XY and Liu HT (2023) Geochronology and geochemistry of early Paleozoic-early Mesozoic magmatic rocks from the Zhangguangcai Range, NE China: Constraints on the tectonic evolution of the eastern Songnen Massif. *Geological Journal* **59**(2), 659–79. https://doi.org/10.1002/gj.4886

Yang DG, Sun DY, Gou J and Hou XG (2017) U-Pb ages of zircons from Mesozoic intrusive rocks in the Yanbian area, Jilin Province, NE China: Transition of the Paleo-Asian oceanic regime to the circum-Pacific tectonic regime. *Journal of Asian Earth Sciences* **143**, 171–90. https://doi.org/10.1016/j.jseaes.2017.04.019

Yang H, Ge WC, Zhao GC, Dong Y, Bi JH, Wang ZH, Yu JJ and Zhang YL (2014) Geochronology and geochemistry of late Pan-African intrusive rocks in the Jiamusi-Khanka Block, NE China: Petrogenesis and geodynamic implications. *Lithos* **208**, 220–36. https://doi.org/10.1016/j.lithos.2014.09.019

Yang JH, Gawood PA, Du YS, Huang H, Huang HW and Tao P (2012) Large Igneous Province and magmatic arc sourced Permian-Triassic volicanogenic sediments in China. *Sedimentary Geology* **261**, 120–31. https://doi.org/10.1016/j.sedgeo.2012.03.018

Yang JH, Wu FY, Shao JA, Wilde SA, Xie LW and Liu XM (2006) Constraints on the timing of uplift of the Yanshan fold and thrust belt, North China. *Earth and Planetary Science Letters* **246**(3-4), 336–52. https://doi.org/10.1016/j.epsl.2006.04.029

Yang JL, Liu FL, Song WM, Yang XP, Wang F and Wang D (2022) Constraints of late Paleoproterozoic granites in Dandong area on Jiao-Liao-Ji Belt orogenesis. *Acta Petrologica Et Mineralogica* **41**(02), 467–90 (in Chinese with English abstract).

Yin CJ, Li DJ, Wang GQ, Hu HX, Dai LX and Zhao J (2011) A probing into the strata position and depositional environment of Kedao Group in Yanbian region from theoretical stratigraphy. *Jilin Geology* **30**(01), 1–9 (in Chinese with English abstract).

Yu HC (2017) A study on the late paleozoic tectonic setting of wangqing area in jilin province. *Jilin University*, Changchun (in Chinese with English abstract).

Yu JJ, Wang F, Xu WL, Gao FH and Tang J (2013) Late Permian tectonic evolution at the southeastern margin of the Songnen-Zhangguangcai range massif, NE China: constraints from geochronology and geochemistry of granitoids. *Gondwana Research* **24**(2), 635–47. https://doi.org/10.1016/j.gr.2012.11.015

Yu SY, Li SZ, Zhang JX, Peng YB, Somerville I, Liu YJ, Wang ZY, Li ZF, Yao Y and Li Y (2019a) Multistage anatexis during tectonic evolution from oceanic subduction to continental collision: A review of the North Qaidam UHP Belt, NW China. *Earth-Science Reviews* **191**: 190–211. https://doi.org/10.1016/j.earscirev.2019.02.016

https://doi.org/10.1017/S0016756824000359 Published online by Cambridge University Press

Yu SY, Li SZ, Zhang JX, Sun DY, Peng YB and Li YS (2019b) Linking high-pressure mafic granulite, TTG-like (tonalitic-trondhjemitic) leucosome and pluton, and crustal growth during continental collision. *The Geological Society of America* **131**, 572–286. https://doi.org/10.1130/B31822.1

Yu SY, Zhang JX, Li SZ, Santosh M, Li YS, Liu YJ, Li XY, Peng YB, Sun DY, Wang ZY and Lv P (2019c) TTG-adakitic-like (Tonalitic-Trondhjemitic) magmas resulting from partial melting of metagabbro under high-pressure condition during continental collision in the North Qaidam UHP Terrane, Western China. *Tectonics* **38**(3), 791–822. https://doi.org/10.1029/2018TC005259

Yu Y, Zong K, Yuan Y, Klemd R, Wang XS, Guo J, Xu R, Hu Z and Liu Y (2022) Crustal Contamination of the Mantle-Derived Liuyuan Basalts: Implications for the Permian Evolution of the Southern Central Asian Orogenic Belt. *Journal of Earth Science* **33**, 1081–94. https://doi.org/10.1007/s12583-022-1706-1

Yuan LL, Zhang XH, Xue FH, Lu YH and Zong KQ (2016) Late Permian high-Mg andesite and basalt association from northern Liaoning, North China: Insights into the final closure of the Paleo-Asian ocean and the orogen-craton boundary. *Lithos* **258**, 58–76. https://doi.org/10.1016/j.lithos.2016.04.024

Zeh A and Gerdes A (2012) U-Pb and Hf isotope record of detrital zircons from gold-bearing sediments of the Pietersburg Greenstone Belt (South Africa)-Is there a common provenance with the witwatersrand basin? *Precambrian Research* **204**, 46–56. https://doi.org/10.1016/j.precamres.2012.02.013

Zhang FQ, Chen HL, Dong CW, Pang YM, Shu P, Wang YL and Yang SF (2008) SHRIMP zircon U-Pb geochronology of volcanic rocks and discussion on the geological time of the Yingcheng Formation of the northern Songliao Basin. *Journal of Stratigraphy* **32**(1), 15–20 (in Chinese with English abstract).

Zhang HH, Qiu L, Yan DP, Zhao ZF, Cai KD, Zhang J, Chen SW, Li YF, Song Y, Zheng YJ, Sun SL, Gong FH and Ariser S (2023) Late-Permian subduction-to-collision transition and closure of Paleo-Asian Ocean in eastern Central Asian Orogenic Belt: Evidence from borehole cores in the Songliao Basin, Northeast China. *Gondwana Research* **122**, 74–92. https://doi.org/10.1016/j.gr.2023.06.004

Zhang JH, Jin W, Wang YF, Zheng PX, Li B and Li CD (2015) Early Archean crustal growth and Re-Melting in the Anshan Area:Evidence from petrology and geochronology of the Eo-Paleoarchean Gneiss complex. *Acta Geologica Sinica* **89**(07), 1195–209 (in Chinese with English abstract).

Zhang L, Liu YJ, Zhang C, Liu XY, Li WM, Ge JT, Liang CY and Zhao YL (2022) Geochronology and geochemistry of the early-middle permian metamorphic volcano-clastic rocks, northern Liaoning Province: Implications for the tectonic evolution of the eastern segment of the northern margin of the North China Craton. *Acta Petrologica Sinica* **38**(8), 2510–38 (in Chinese with English abstract). https://doi.org/10.18654/1000-0569/2022.08.15

Zhang Q, Liang CY, Liu YJ, Zheng CQ and Li WM (2019) Final Closure Time of the Paleo-Asian Ocean: Implication from the provenance transformation from the Yangjiagou formation to Lujiatun formation in the Jiutai Area, NE China. *Acta Geologica Sinica* (Eng) **93**, 1456–76. https://doi.org/10.1111/1755-6724.14388

Zhang XH, Wang YS, Zang XY, Li AP, Li YF, Liu XS, Liu HL and Li B (2021) Early Paleozoic northward subduction records of Paleo-Asian Ocean: zircon U-Pb geochronological and geochemical evidence from early Silurian island-arc volcanic rocks in central Jilin Province. *Global Geology* **40**(04), 759–71 (in Chinese with English abstract).

Zhang YB, Wu FY, Wilde SA, Zhai MG, Lu XP and Sun DY (2004) Zircon U-Pb ages and tectonic implications of 'Early Paleozoic' granitoids at Yanbian, Jilin Province, northeast China. *Island Arc* **13**, 484–505. https://doi.org/10.1111/j.1440-1738.2004.00442.x

Zhang ZJ, Xing SW, Ma YB, Du XH, Sun JG, Huang MR and Cui DY (2013) Zircon U-Pb dating of the biotite-bearing plagioclase amphibolite from hongtoushan Cu-Zn deposit,Liaoning Province,China and its implications on the exploration of VMS. *Journal of Jilin University (Earth Science Edition)* **43**(04), 1159–68 (in Chinese with English abstract). https://doi.org/10.13278/j.cnki.jjuese.2013.04.027

Zhao GC, Cawood PA, Li SZ, Wilde SA, Sun M, Zhang J, He YH and Yin CQ (2012) Amalgamation of the North China Craton: Key issues and discussion. *Precambrian Research* **222**, 55–76. https://doi.org/10.1016/j.precamres.2012.09.016

Zhao LL, Xu FZ, Zhang Y, Ni B and Ma XH (2021) Zircon U-Pb chronology of the Heilongjiang complex in Mudanjiang area: Geological implication. *Geology and Resources* **30**(04), 405–13 (in Chinese with English abstract). https://doi.org/10.13686/j.cnki.dzyzy.2021.04.001

Zhao P, Chen Y, Xu B, Faure M, Shi GZ and Choulet F (2013) Did the Paleo-Asian Ocean between north China block and Mongolia block exist during the late Paleozoic? First paleomagnetic evidence from central-eastern inner Mongolia, China. *Journal of Geophysical Research: Solid Earth* **118**, 1873–94. https://doi.org/10.1002/jgrb.50198

Zhao Q, Tang JR, Yang HY, Zhang XL and Luo LJ (2023) Geochronology and geochemistry of late Triassic Adakite in the Central Jiamusi Block, China and their geological significance. *Journal of Earth Sciences and Environment* **45**(2), 240–55 (in Chinese with English abstract). https://doi.org/10.19814/j.jese.2022.02007

Zhou JB, Jie H, Wilde SA and Guo XD (2013) A primary study of the Jilin-Heilongjiang high-pressure metamorphic belt: Evidence and tectonic implications. *Acta Petrologica Sinica* **29**, 386–98 (in Chinese with English abstract).

Zhou JB, Wang B, Wilde SA, Zhao GC, Cao JL, Zheng CQ and Zeng WS (2015) Geochemistry and U-Pb zircon dating of the Toudaoqiao blueschists in the Great Xing'an Range, northeast China, and tectonic implications. *Journal of Asian Earth Sciences* **97**, 197–210. https://doi.org/10.1016/j.jseaes.2014.07.011

Zhou JB and Wilde SA (2013) The crustal accretion history and tectonic evolution of the NE China segment of the Central Asian Orogenic Belt. *Gondwana Research* **23**, 1365–77. https://doi.org/10.1016/j.gr.2012.05.012

Zhou JB, Wilde SA, Zhang XZ, Ren SM and Zheng CQ (2011a) Early Paleozoic metamorphic rocks of the Erguna block in the Great Xing'an Range, NE China: Evidence for the timing of magmatic and metamorphic events and their tectonic implications. *Tectonophysics* **499**, 105117. https://doi.org/10.1016/j.tecto.2010.12.009

Zhou JB, Wilde SA, Zhang XZ, Zhao GC, Zheng CQ, Wang YJ and Zhang XH (2009) The onset of Pacific margin accretion in NE China: evidence from the Heilongjiang high-pressure metamorphic belt. *Tectonophysics* **478**, 230–46. https://doi.org/10.1016/j.tecto.2009.08.009

Zhou JB, Wilde SA, Zhao GC and Han J (2018) Nature and assembly of microcontinental blocks within the Paleo Asian Ocean. *Earth Science Reviews* **186**, 76–93. https://doi.org/10.1016/j.earscirev.2017.01.012

Zhou JB, Zhang XZ, Wilde SA and Zheng CQ (2011b) Confirming of the Heilongjiang ~500Ma Pan-African khondalite belt and its tectonic implications. *Acta Petrologica Sinica* **27**(4), 1235–45 (in Chinese with English abstract).

Zhou XD (2009) Early Carboniferous to Early Triassic Stratigraphic Sequence and tectonic evolution in central and eastern Jilin. *Jilin University*, Changchun (in Chinese with English abstract).

Zhou ZB, Pei FP, Wang ZW, Cao HH, Xu WL, Wang ZJ and Zhang Y (2017) Using detrital zircons from late Permian to Triassic sedimentary rocks in the south-eastern Central Asian Orogenic Belt (NE China) to constrain the timing of the final closure of the Paleo-Asian Ocean. *Journal of Asian Earth Sciences* **144**, 82–109. https://doi.org/10.1016/j.jseaes.2016.12.007

Zhu JB and Ren JS (2017) Carboniferous-permian stratigraphy and sedimentary environment of Southeastern inner Mongolia, China: Constraints on final closure of the Paleo-Asian Ocean. *Acta Geologica Sinica (English Edition)* **91**, 832–56. https://doi.org/10.1111/1755-6724.13313